APOBEC3G-mediated G-to-A mutations in HIV-1 evolution and drug resistance. PLoS Pathog. 5:e1000367.
19. **Kawano, Y., Y. Tanaka, N. Misawa, R. Tanaka, J. I. Kira, T. Kimura, M. Fukushi, K. Sano, T. Goto, M. Nakai, T. Kobayashi, N. Yamamoto, and Y. Koyanagi.** 1997. Mutational analysis of human immunodeficiency virus type 1 (HIV-1) accessory genes: requirement of a site in the *nef* gene for HIV-1 replication in activated $CD4^+$ T cells in vitro and in vivo. J. Virol. **71**:8456–8466.
20. **Kieffer, T. L., P. Kwon, R. E. Nettles, Y. Han, S. C. Ray, and R. F. Siliciano.** 2005. G→A hypermutation in protease and reverse transcriptase regions of human immunodeficiency virus type 1 residing in resting $CD4^+$ T cells in vivo. J. Virol. **79**:1975–1980.
21. **Kobayashi, M., A. Takaori-Kondo, Y. Miyauchi, K. Iwai, and T. Uchiyama.** 2005. Ubiquitination of APOBEC3G by an HIV-1 Vif-Cullin5-Elongin B-Elongin C complex is essential for Vif function. J. Biol. Chem. **280**:18573–18578.
22. **Koyanagi, Y., S. Miles, R. T. Mitsuyasu, J. E. Merrill, H. V. Vinters, and I. S. Chen.** 1987. Dual infection of the central nervous system by AIDS viruses with distinct cellular tropisms. Science **236**:819–822.
23. **Land, A. M., T. B. Ball, M. Luo, R. Pilon, P. Sandstrom, J. E. Embree, C. Wachihi, J. Kimani, and F. A. Plummer.** 2008. Human immunodeficiency virus (HIV) type 1 proviral hypermutation correlates with CD4 count in HIV-infected women from Kenya. J. Virol. **82**:8172–8182.
24. **Langlois, M. A., R. C. Beale, S. G. Conticello, and M. S. Neuberger.** 2005. Mutational comparison of the single-domained APOBEC3C and double-domained APOBEC3F/G anti-retroviral cytidine deaminases provides insight into their DNA target site specificities. Nucleic Acids Res. **33**:1913–1923.
25. **Lecossier, D., F. Bouchonnet, F. Clavel, and A. J. Hance.** 2003. Hypermutation of HIV-1 DNA in the absence of the Vif protein. Science **300**:1112.
26. **Li, Y., J. C. Kappes, J. A. Conway, R. W. Price, G. M. Shaw, and B. H. Hahn.** 1991. Molecular characterization of human immunodeficiency virus type 1 cloned directly from uncultured human brain tissue: identification of replication-competent and -defective viral genomes. J. Virol. **65**:3973–3985.
27. **Liddament, M. T., W. L. Brown, A. J. Schumacher, and R. S. Harris.** 2004. APOBEC3F properties and hypermutation preferences indicate activity against HIV-1 in vivo. Curr. Biol. **14**:1385–1391.
28. **Luo, K., T. Wang, B. Liu, C. Tian, Z. Xiao, J. Kappes, and X. F. Yu.** 2007. Cytidine deaminases APOBEC3G and APOBEC3F interact with human immunodeficiency virus type 1 integrase and inhibit proviral DNA formation. J. Virol. **81**:7238–7248.
29. **Mangeat, B., P. Turelli, G. Caron, M. Friedli, L. Perrin, and D. Trono.** 2003. Broad antiretroviral defence by human APOBEC3G through lethal editing of nascent reverse transcripts. Nature **424**:99–103.
30. **Mansky, L. M., and H. M. Temin.** 1995. Lower in vivo mutation rate of human immunodeficiency virus type 1 than that predicted from the fidelity of purified reverse transcriptase. J. Virol. **69**:5087–5094.
31. **Marin, M., K. M. Rose, S. L. Kozak, and D. Kabat.** 2003. HIV-1 Vif protein binds the editing enzyme APOBEC3G and induces its degradation. Nat. Med. **9**:1398–1403.
32. **Mbisa, J. L., R. Barr, J. A. Thomas, N. Vandegraaff, I. J. Dorweiler, E. S. Svarovskaia, W. L. Brown, L. M. Mansky, R. J. Gorelick, R. S. Harris, A. Engelman, and V. K. Pathak.** 2007. Human immunodeficiency virus type 1 cDNAs produced in the presence of APOBEC3G exhibit defects in plus-strand DNA transfer and integration. J. Virol. **81**:7099–7110.
33. **Mulder, L. C., A. Harari, and V. Simon.** 2008. Cytidine deamination induced HIV-1 drug resistance. Proc. Natl. Acad. Sci. U. S. A. **105**:5501–5506.
34. **Nie, C., K. Sato, N. Misawa, H. Kitayama, H. Fujino, H. Hiramatsu, T. Heike, T. Nakahata, Y. Tanaka, M. Ito, and Y. Koyanagi.** 2009. Selective infection of $CD4^+$ effector memory T lymphocytes leads to preferential depletion of memory T lymphocytes in R5 HIV-1-infected humanized NOD/SCID/IL-2Rγ^{null} mice. Virology **394**:64–72.
35. **Nowarski, R., E. Britan-Rosich, T. Shiloach, and M. Kotler.** 2008. Hypermutation by intersegmental transfer of APOBEC3G cytidine deaminase. Nat. Struct. Mol. Biol. **15**:1059–1066.
36. **Pace, C., J. Keller, D. Nolan, I. James, S. Gaudieri, C. Moore, and S. Mallal.** 2006. Population level analysis of human immunodeficiency virus type 1 hypermutation and its relationship with APOBEC3G and vif genetic variation. J. Virol. **80**:9259–9269.
37. **Palmer, S., M. Kearney, F. Maldarelli, E. K. Halvas, C. J. Bixby, H. Bazmi, D. Rock, J. Falloon, R. T. Davey, Jr., R. L. Dewar, J. A. Metcalf, S. Hammer, J. W. Mellors, and J. M. Coffin.** 2005. Multiple, linked human immunodeficiency virus type 1 drug resistance mutations in treatment-experienced patients are missed by standard genotype analysis. J. Clin. Microbiol. **43**:406–413.
38. **Pathak, V. K., and H. M. Temin.** 1990. Broad spectrum of *in vivo* forward mutations, hypermutations, and mutational hotspots in a retroviral shuttle vector after a single replication cycle: substitutions, frameshifts, and hypermutations. Proc. Natl. Acad. Sci. U. S. A. **87**:6019–6023.
39. **Piantadosi, A., D. Humes, B. Chohan, R. S. McClelland, and J. Overbaugh.** 2009. Analysis of the percentage of human immunodeficiency virus type 1 sequences that are hypermutated and markers of disease progression in a longitudinal cohort, including one individual with a partially defective Vif. J. Virol. **83**:7805–7814.
40. **Pillai, S. K., J. K. Wong, and J. D. Barbour.** 2008. Turning up the volume on mutational pressure: is more of a good thing always better? (A case study of HIV-1 Vif and APOBEC3.) Retrovirology **5**:26.
41. **Russell, R. A., M. D. Moore, W. S. Hu, and V. K. Pathak.** 2009. APOBEC3G induces a hypermutation gradient: purifying selection at multiple steps during HIV-1 replication results in levels of G-to-A mutations that are high in DNA, intermediate in cellular viral RNA, and low in virion RNA. Retrovirology **6**:16.
42. **Salazar-Gonzalez, J. F., E. Bailes, K. T. Pham, M. G. Salazar, M. B. Guffey, B. F. Keele, C. A. Derdeyn, P. Farmer, E. Hunter, S. Allen, O. Manigart, J. Mulenga, J. A. Anderson, R. Swanstrom, B. F. Haynes, G. S. Athreya, B. T. Korber, P. M. Sharp, G. M. Shaw, and B. H. Hahn.** 2008. Deciphering human immunodeficiency virus type 1 transmission and early envelope diversification by single-genome amplification and sequencing. J. Virol. **82**:3952–3970.
43. **Sato, K., J. Aoki, N. Misawa, E. Daikoku, K. Sano, Y. Tanaka, and Y. Koyanagi.** 2008. Modulation of human immunodeficiency virus type 1 infectivity through incorporation of tetraspanin proteins. J. Virol. **82**:1021–1033.
44. **Sato, K., S. P. Yamamoto, N. Misawa, T. Yoshida, T. Miyazawa, and Y. Koyanagi.** 2009. Comparative study on the effect of human BST-2/Tetherin on HIV-1 release in cells of various species. Retrovirology **6**:53.
45. **Sheehy, A. M., N. C. Gaddis, and M. H. Malim.** 2003. The antiretroviral enzyme APOBEC3G is degraded by the proteasome in response to HIV-1 Vif. Nat. Med. **9**:1404–1407.
46. **Shindo, K., A. Takaori-Kondo, M. Kobayashi, A. Abudu, K. Fukunaga, and T. Uchiyama.** 2003. The enzymatic activity of CEM15/Apobec-3G is essential for the regulation of the infectivity of HIV-1 virion but not a sole determinant of its antiviral activity. J. Biol. Chem. **278**:44412–44416.
47. **Shirakawa, K., A. Takaori-Kondo, M. Kobayashi, M. Tomonaga, T. Izumi, K. Fukunaga, A. Sasada, A. Abudu, Y. Miyauchi, H. Akari, K. Iwai, and T. Uchiyama.** 2006. Ubiquitination of APOBEC3 proteins by the Vif-Cullin5-ElonginB-ElonginC complex. Virology **344**:263–266.
48. **Simmonds, P., P. Balfe, C. A. Ludlam, J. O. Bishop, and A. J. Brown.** 1990. Analysis of sequence diversity in hypervariable regions of the external glycoprotein of human immunodeficiency virus type 1. J. Virol. **64**:5840–5850.
49. **Simon, V., V. Zennou, D. Murray, Y. Huang, D. D. Ho, and P. D. Bieniasz.** 2005. Natural variation in Vif: differential impact on APOBEC3G/3F and a potential role in HIV-1 diversification. PLoS Pathog. **1**:e6.
50. **Stopak, K., C. de Noronha, W. Yonemoto, and W. C. Greene.** 2003. HIV-1 Vif blocks the antiviral activity of APOBEC3G by impairing both its translation and intracellular stability. Mol. Cell **12**:591–601.
51. **Suspene, R., C. Rusniok, J. P. Vartanian, and S. Wain-Hobson.** 2006. Twin gradients in APOBEC3 edited HIV-1 DNA reflect the dynamics of lentiviral replication. Nucleic Acids Res. **34**:4677–4684.
52. **Tanaka, Y., H. Marusawa, H. Seno, Y. Matsumoto, Y. Ueda, Y. Kodama, Y. Endo, J. Yamauchi, T. Matsumoto, A. Takaori-Kondo, I. Ikai, and T. Chiba.** 2006. Anti-viral protein APOBEC3G is induced by interferon-α stimulation in human hepatocytes. Biochem. Biophys. Res. Commun. **341**:314–319.
53. **Ulenga, N. K., A. D. Sarr, D. Hamel, J. L. Sankale, S. Mboup, and P. J. Kanki.** 2008. The level of APOBEC3G (hA3G)-related G-to-A mutations does not correlate with viral load in HIV type 1-infected individuals. AIDS Res. Hum. Retroviruses **24**:1285–1290.
54. **Vartanian, J. P., M. Henry, and S. Wain-Hobson.** 2002. Sustained G→A hypermutation during reverse transcription of an entire human immunodeficiency virus type 1 strain Vau group O genome. J. Gen. Virol. **83**:801–805.
55. **Vartanian, J. P., A. Meyerhans, B. Asjo, and S. Wain-Hobson.** 1991. Selection, recombination, and G→A hypermutation of human immunodeficiency virus type 1 genomes. J. Virol. **65**:1779–1788.
56. **Wiegand, H. L., B. P. Doehle, H. P. Bogerd, and B. R. Cullen.** 2004. A second human antiretroviral factor, APOBEC3F, is suppressed by the HIV-1 and HIV-2 Vif proteins. EMBO J. **23**:2451–2458.
57. **Wood, N., T. Bhattacharya, B. F. Keele, E. Giorgi, M. Liu, B. Gaschen, M. Daniels, G. Ferrari, B. F. Haynes, A. McMichael, G. M. Shaw, B. H. Hahn, B. Korber, and C. Seoighe.** 2009. HIV evolution in early infection: selection pressures, patterns of insertion and deletion, and the impact of APOBEC. PLoS Pathog. **5**:e1000414.
58. **Yu, Q., D. Chen, R. Konig, R. Mariani, D. Unutmaz, and N. R. Landau.** 2004. APOBEC3B and APOBEC3C are potent inhibitors of simian immunodeficiency virus replication. J. Biol. Chem. **279**:53379–53386.
59. **Yu, Q., R. Konig, S. Pillai, K. Chiles, M. Kearney, S. Palmer, D. Richman, J. M. Coffin, and N. R. Landau.** 2004. Single-strand specificity of APOBEC3G accounts for minus-strand deamination of the HIV genome. Nat. Struct. Mol. Biol. **11**:435–442.
60. **Yu, X., Y. Yu, B. Liu, K. Luo, W. Kong, P. Mao, and X. F. Yu.** 2003. Induction of APOBEC3G ubiquitination and degradation by an HIV-1 Vif-Cul5-SCF complex. Science **302**:1056–1060.
61. **Zhang, H., B. Yang, R. J. Pomerantz, C. Zhang, S. C. Arunachalam, and L. Gao.** 2003. The cytidine deaminase CEM15 induces hypermutation in newly synthesized HIV-1 DNA. Nature **424**:94–98.

JOURNAL OF VIROLOGY, June 2010, p. 6082–6095 Vol. 84, No. 12
0022-538X/10/$12.00 doi:10.1128/JVI.02516-09

Persistence of Viremia and Production of Neutralizing Antibodies Differentially Regulated by Polymorphic *APOBEC3* and *BAFF-R* Loci in Friend Virus-Infected Mice▽

Sachiyo Tsuji-Kawahara,[1] Tomomi Chikaishi,[1,2] Eri Takeda,[1]† Maiko Kato,[1,3] Saori Kinoshita,[1] Eiji Kajiwara,[1] Shiki Takamura,[1] and Masaaki Miyazawa[1]*

Departments of Immunology[1] and Dermatology,[3] Kinki University School of Medicine, 377-2 Ohno-Higashi, Osaka-Sayama, Osaka 589-8511, Japan, and UMN Pharma Inc., Yokohama 222-0033, Japan[2]

Received 30 November 2009/Accepted 26 March 2010

Several host genes control retroviral replication and pathogenesis through the regulation of immune responses to viral antigens. The *Rfv3* gene influences the persistence of viremia and production of virus-neutralizing antibodies in mice infected with Friend mouse retrovirus complex (FV). This locus has been mapped within a narrow segment of mouse chromosome 15 harboring the *APOBEC3* and *BAFF-R* loci, both of which show functional polymorphisms among different strains of mice. The exon 5-lacking product of the *APOBEC3* allele expressed in FV-resistant C57BL/6 (B6) mice directly restricts viral replication, and mice lacking the B6-derived *APOBEC3* exhibit exaggerated pathology and reduced production of neutralizing antibodies. However, the mechanisms by which the polymorphisms at the *APOBEC3* locus affect the production of neutralizing antibodies remain unclear. Here we show that the *APOBEC3* genotypes do not directly affect the B-cell repertoire, and mice lacking B6-derived *APOBEC3* still produce FV-neutralizing antibodies in the presence of primed T helper cells. Instead, higher viral loads at a very early stage of FV infection caused by either a lack of the B6-derived *APOBEC3* or a lack of the wild-type *BAFF-R* resulted in slower production of neutralizing antibodies. Indeed, B cells were hyperactivated soon after infection in the *APOBEC3*- or *BAFF-R*-deficient mice. In contrast to mice deficient in the B6-derived *APOBEC3*, which cleared viremia by 4 weeks after FV infection, mice lacking the functional *BAFF-R* allele exhibited sustained viremia, indicating that the polymorphisms at the *BAFF-R* locus may better explain the *Rfv3*-defining phenotype of persistent viremia.

Several host genetic factors control retroviral replication and pathogenesis through the regulation of immune responses to viral antigens. The recovery from Friend virus 3 gene (*Rfv3*) was identified as a host gene locus that affects the persistence of viremia and development of virus-specific antibody (Ab) responses upon Friend virus (FV) infection (5). FV is the pathogenic retrovirus complex composed of replication-competent Friend murine leukemia virus (F-MuLV) and the defective spleen focus-forming virus (SFFV). The product of the SFFV *env* gene, gp55, forms a complex with the erythropoietin receptor and the short form of the hematopoietic-cell-specific receptor tyrosine kinase (STK), and this interaction induces the growth and terminal differentiation of erythroid progenitor cells, causing increased hematocrit values and massive splenomegaly. The resultant increase in targets of FV integration consequently causes the emergence of mono- or oligoclonal erythroleukemia through insertional activation of transcription factors or disruption of a tumor suppressor gene (15, 29, 34). Mice of the C57BL background possess mutations in the intron of the *Stk* gene and lack expression of the short-form STK, resulting in resistance to SFFV-induced splenomegaly (37). This host factor was first described as polymorphisms at the *Fv2* locus, with the resistance allele found in C57BL mice being designated the recessive $Fv2^r$ (21).

The *Rfv3* gene was originally described based on the segregation of FV-induced leukemia development from persistence of viremia (5). (B10.A × A/WySn)F_1 and A/WySn mice both developed leukemia after FV infection due to their shared susceptible major histocompatibility complex (MHC) haplotype, $H2^a$. However, despite the common trait of susceptibility to leukemia development, most of the (B10.A × A/WySn)F_1 mice had cleared viremia by 30 to 50 days after FV inoculation, while the majority of A/WySn mice remained viremic. As one-half of the (B10.A × A/WySn)F_1 × A/WySn backcross mice had cleared viremia by 30 to 50 days after FV inoculation, a single gene affecting the persistence of viremia was postulated and designated *Rfv3* (5). When crosses of $H2^b$ mice were similarly analyzed, it was found that most of the A.BY mice remained viremic at 30 to 60 days after FV infection and developed leukemia, while (C57BL/10 × A.BY)F_1 mice cleared viremia and showed resistance to leukemia development. Again, about one-half of the (C57BL/10 × A.BY)F_1 × A.BY backcross mice remained viremic at 30 to 60 days postinfection, and a slightly larger fraction developed leukemia (4, 5). These results indicate that clearance of viremia in the presence of the C57BL-derived dominant *Rfv3* genotype is a prerequisite for resistance against FV-induced leukemia development, and $H2^b$ mice can show a low incidence of leukemia provided that they possess the resistant *Rfv3* genotype and clear viremia (4). Since BALB.B mice remained viremic at 30 to 50 days

* Corresponding author. Mailing address: Department of Immunology, Kinki University School of Medicine, 377-2 Ohno-Higashi, Osaka-Sayama, Osaka 589-8511, Japan. Phone and fax: 81-72-367-7660. E-mail: masaaki@med.kindai.ac.jp.
† Present address: Viral Infectious Disease Unit, RIKEN, Wako, Saitama 351-0198, Japan.
▽ Published ahead of print on 7 April 2010.

after FV infection (5), it has been postulated that C57BL/6 (B6) and C57BL/10 mice possess the dominant *Rfv3*^{r} genotype, which confers early clearance of viremia, while A.BY, A/WySn, and BALB.B mice share the recessive *Rfv3*^{s} genotype, associated with persistence of viremia irrespective of their *H2* haplotypes (4). These *Rfv3* genotypes were later associated with the production of anti-FV Abs capable of lysing FV-induced leukemia cells and a reduction in cell surface expression of FV antigens on spleen cells in *Rfv3*^{r} mice (9), suggesting that the *Rfv3* gene might regulate the production of anti-FV Abs. The location of the *Rfv3* gene was narrowed down to a segment of mouse chromosome 15 by comparing levels of viremia at 30 days after FV infection in (B10.A × A/WySn)F_1 × A/WySn backcross and (B10.A × A/WySn)F_2 mice (12, 48). We took a separate approach and examined the titers of virus-neutralizing Abs in (B10.A × A/WySn)F_1 × A/WySn backcross mice (16). By analyses of linkages between polymorphic markers and titers of FV-neutralizing Abs at postinoculation day (PID) 15, the *Rfv3* locus was again mapped within a narrow segment of chromosome 15 (16). We further compared the expression levels, after FV infection, of all the candidate genes between the *Rfv3*$^{r/s}$ and *Rfv3*$^{s/s}$ mice (29), and polymorphisms at the apolipoprotein B mRNA-editing enzyme catalytic polypeptide-like editing complex 3 locus (*APOBEC3*) have recently been associated with the levels of viremia or restricted replication of FV by two independent research groups (43, 49).

The major transcript of the *APOBEC3* allele expressed in FV-resistant B6 mice lacks exon 5 (Δ5), and the product of this *mA3*^{b} allele highly restricts FV replication both *in vitro* and *in vivo* (49). On the other hand, BALB/c and A strains of mice express the full-length and Δ5 transcripts from their *mA3*^{d} allele; the translated products of both poorly inhibit the replication of an infectious F-MuLV clone. An additional allelic difference is that the expression levels of *mA3*^{b} are significantly higher than those of the *mA3*^{d} allele (36, 49). Thus, a lack of expression of the resistance-associated *mA3*^{b} allele in gene-targeted mice and their hybrids resulted in 100- to 1,000-fold-higher levels of FV replication and higher hematocrit values (49). Additionally, reduced levels of virus-neutralizing Abs were observed in mice lacking the *mA3*^{b} allele (43). However, the mechanisms by which the polymorphisms at the *APOBEC3* locus, which encodes the intracellular cytidine deaminase protein, may affect the production of virus-neutralizing Abs remain unclear. Further, the relationship between the production of virus-neutralizing Abs and control of viremia also remains uncertain, as the reduction in the number of virus-producing cells can be observed prior to the detection of virus-neutralizing Abs in the serum of vaccinated animals (17, 27). The possible causative relationships between the production of virus-neutralizing Abs and clearance of viremia are important, especially because the original *Rfv3* phenotypes were defined by the persistence of viremia at PIDs >30 (4, 5), while the polymorphisms in the genetic markers linked with the *APOBEC3* locus affect serum titers of virus-neutralizing Abs at PID 15 (16).

Of note, A/WySn mice, which were used to identify *Rfv3* as a single gene locus (4, 5), but not A/J mice are known to possess a natural mutation in the receptor for B-cell-activating factor belonging to the TNF family (BAFF-R), which results in reduced size of the peripheral B-cell compartment and attenuation of antigen-specific IgG responses (1, 51). The structural gene for this receptor, *BAFF-R*, is located in chromosome 15, only about 2 megabase pairs telomeric to the *APOBEC3* locus. A/WySn mice harbor a 4.7-kb insertion in exon 3 of this gene (35, 51). Both differentiation and maturation phenotypes and functions of B cells in A/WySn mice are essentially similar to those observed in mice with a targeted disruption of the *BAFF-R* gene, in which both immature and mature peripheral B cells exhibit shorter half-lives (20, 39, 44, 45). As the genetic mapping of the *Rfv3* locus has been performed by using A/WySn mice or their progeny obtained by crossing them with B10.A mice (12, 16, 48), there remains the possibility that the polymorphism at the *BAFF-R* locus in close linkage with the *APOBEC3* genotypes may have affected the *Rfv3* phenotypes. We report here that polymorphisms at the *APOBEC3* and *BAFF-R* loci independently influence the production of virus-neutralizing Abs upon FV infection. We further propose a possible mechanism by which the *APOBEC3* alleles affect F-MuLV-specific Ab responses.

MATERIALS AND METHODS

Mice and virus. C57BL/6 CrSlc and A/J JmsSlc mice were purchased from Japan SLC, Inc., Hamamatsu, Japan. A/WySnJ and B6(Cg)-*Tnfrsf13c*^{tm1Mass}/J (B6-*BAFF-R*$^{-/-}$) mice were purchased from The Jackson Laboratory, Bar Harbor, ME. The B6-*BAFF-R*$^{-/-}$ mice homozygously carry a targeted disruption of the *BAFF-R* gene (44). The APOBEC3-deficient mice on a B6 background (B6-*mA3*$^{-/-}$) have been described previously (26, 49). Mice 7 to 10 weeks old were used throughout the present study. All animals were housed and bred in the Experimental Animal Facilities at Kinki University School of Medicine under specific-pathogen-free conditions, and all animal experiments were conducted according to the guidelines of Kinki University. A stock of B-tropic FV complex without contamination of lactate dehydrogenase-elevating virus has been described previously (49). Replication-competent helper virus of the FV, F-MuLV, was purified from the culture supernatant of *Mus dunni* cells persistently infected with infectious molecular clone FB29 (46).

Assays for plasma viral load. Mice were bled from the buccal vein with an 18-gauge needle under ether anesthesia, and the plasma was separated and stored at −30°C until use. Serial 3-fold dilutions of plasma were loaded in the presence of 4 μg/ml Polybrene (Sigma-Aldrich Corp., St. Louis, MO) on monolayers of *Mus dunni* cells that had been seeded at 1.0×10^4 cells per well of 24-well plates on the previous day in RPMI 1640 supplement with 10% fetal bovine serum (FBS). Two days later, the cells were washed twice with phosphate-buffered balanced salt solution (PBBS) and fixed with methanol. F-MuLV-infected cell foci were stained with monoclonal Ab (MAb) 720 (41), which detects the F-MuLV *env* gene product, and visualized by using biotinylated anti-mouse immunoglobulin (Ig) Ab and avidin-biotinylated peroxidase complex (Vector Laboratories, Burlingame, CA) as described previously (17, 27, 41). The foci were counted under a magnifier, and the F-MuLV titers of plasma samples were calculated as focus-forming units (FFU) per ml.

Assays for virus-neutralizing Abs. The *in vitro* assays for quantitative measurement of F-MuLV-neutralizing Abs have been described elsewhere in detail (17, 27, 47). Mice were bled, and the sera were separated and heat inactivated at 56°C for 30 min. As demonstrated previously (19), this heating procedure inactivates most of the remaining infectivity due to viremia, if there is any, in serum samples, which we also confirmed (data not shown). Serial 2-fold dilutions of sera were mixed with 100 FFU of the F-MuLV stock virus. The virus/antibody mixtures were added onto cultured *Mus dunni* cells, and F-MuLV-infected cell foci were counted as described in the protocol for the plasma viremia assay. The virus mixed with PBBS was added to control wells. Neutralizing titers were calculated as the logarithm of maximum dilutions that gave a reduction in the number of F-MuLV-infected cell foci to <25% of those in the control wells. IgG titers were determined by treating each serum with 2-mercaptoethanol (17).

Northern blot analyses and quantitative real-time PCR assays. Northern blot analyses and quantitative real-time PCR assays were performed with total RNA prepared from various mouse tissues or cells to determine *APOBEC3* mRNA expression as described previously using the same primers and probes (49). $CD19^+$ B cells and $CD3^+$ T cells were separated from the spleens of B6 mice by using MAb-conjugated magnetic microbeads (Miltenyi Biotec GmbH, Germany)

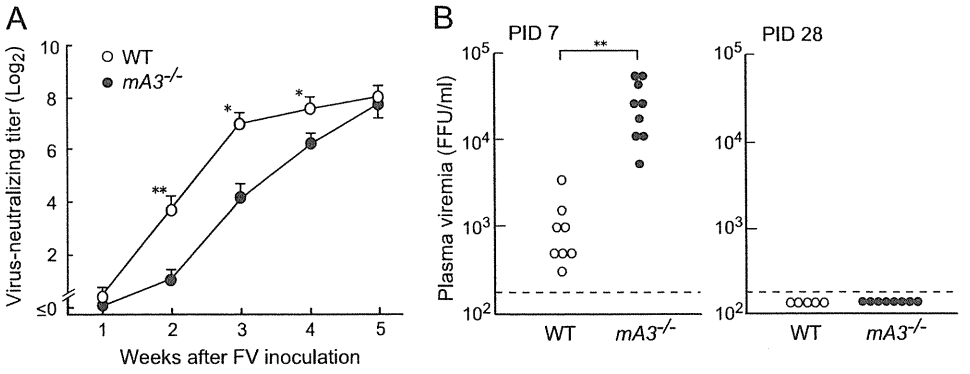

FIG. 1. Kinetics of virus-neutralizing Ab production and levels of plasma viremia in B6 mice lacking the $mA3^b$ allele upon FV infection. The $mA3^{-/-}$ and WT B6 mice were inoculated with 10,000 spleen focus-forming units (SFFU) of FV. (A) Sera were collected weekly for 5 weeks, and titers of Abs capable of neutralizing an infectious molecular clone of F-MuLV were measured by focal immunoassay. Neutralizing titers were determined as serum dilutions causing a 75% reduction in the infectivity. Each data point represents the mean titer of IgG plus IgM calculated with 5 to 9 separate serum samples ± standard error of the mean (SEM). One-way ANOVA for repeated measures with Bonferroni post hoc tests was used to calculate P values (*, $P < 0.05$; **, $P < 0.005$). (B) Levels of plasma viremia were measured at PIDs 7 and 28. Each dot represents the level of FV viremia for an individual mouse as detected by focal immunoassay using *Mus dunni* cells. The limit of detection was 200 FFU/ml. **, $P < 0.005$ by Student's t test.

according to the manufacturer's instructions. For the Northern blot analysis, 2 micrograms of total RNA was separated in a 1% formaldehyde-agarose gel and visualized by ethidium bromide staining. The mRNA encoding β-actin was used as an internal control. For the quantitative real-time PCR assays, the expression levels of mouse *GAPDH* mRNA were used as an internal control. The ΔC_T values were determined by subtracting the average threshold cycle (C_T) value for *GAPDH* from the average C_T value for *APOBEC3*. The relative expression levels of the *APOBEC3* mRNA in each cell population were then determined as $\Delta\Delta C_T$ values relative to the ΔC_T values obtained with the whole spleen cells.

Immunization and enzyme-linked immunosorbent assay (ELISA). Mice were injected intraperitoneally with 100 μg of 2,4-dinitrophenylated (DNP) ovalbumin (DNP-OVA; Biosearch Technologies, Novato, CA) in alum and boosted once with 50 μg of DNP-OVA without alum at an interval of 10 days. The mice were bled before or at 7 days after the last immunization, and the sera were separated. T-cell-independent responses were elicited by intraperitoneal injection of 100 μg DNP-Ficoll (Biosearch Technologies). The serum Abs were captured on plates coated with DNP-conjugated keyhole limpet hemocyanin; they were then detected by incubation with peroxidase-conjugated rabbit anti-mouse IgM (μ-chain specific) or anti-mouse IgG (γ-chain specific), both purchased from Zymed Laboratories (San Francisco, CA), followed by an incubation with benzidine as a chromogen (Sigma-Aldrich). Relative Ab titers were determined by comparing values of optical density at 405 nm (OD_{405}) with those obtained with an appropriate dilution of standard mouse IgM or IgG captured onto goat anti-mouse Ig-coated plates.

Peptide synthesis and immunization. Peptide i, representing a single T-helper-cell epitope encoded by the F-MuLV *env* gene (gp70 residues 462 to 479) (27), was purchased from Operon Biotechnologies (Tokyo, Japan). For immunization, the lyophilized peptide was dissolved in PBBS and emulsified with an equal volume of complete Freund's adjuvant (CFA; Difco Laboratories, Detroit, MI). Mice were immunized once subcutaneously in the abdominal wall with multiple split doses for a total of 100 μl of the emulsion containing 10 μg of the peptide. Three weeks later, they were challenged with FV complex as described previously (17, 27). The control mice were given the same amount of CFA emulsified with PBBS. FV-induced pathology was assessed by monitoring hematocrit values, and spleen weights were measured at 77 days after FV infection.

Flow cytometry. Flow cytometric analyses of cell surface markers were performed as described elsewhere (17, 47). Spleen cell suspensions were stained with the following MAbs conjugated with fluorescein isothiocyanate (FITC), phycoerythrin (PE), PerCP-Cy5.5, allophycocyanin, or biotin: anti-mouse CD19, anti-mouse CD69, anti-mouse TER-119, anti-mouse IgD (δ-chain specific), and anti-mouse IgM (μ-chain specific), all purchased from BD Biosciences. F-MuLV-infected cells were detected with biotinylated MAb 720 as described previously (17). Data were acquired with a FACSCalibur (BD Biosciences, Franklin Lakes, NJ) and were analyzed with CELLQuest Pro software.

Genotyping. Mouse genomic DNA was prepared from the tails as described previously (16). *BAFF-R* genotypes were determined by PCR analyses using the oligonucleotide primers 5′-CACCATGGGCGCCAGGAGACTC-3′ (for both B6- and A/WySn-derived alleles) and 5′-GAAGTCCACAAGCCCAGTAGAG AT-3′ (for the B6-derived allele) or 5′-ACGTTCACGGGAAAAACAGAGT-3′ (for the A/WySn-derived allele). For determination of the *APOBEC3* genotypes, a genomic region harboring intron 4 of *APOBEC3*, in which there are sequence polymorphisms between the two strains of mice (36), was amplified using the primers 5′-AATTTAAAAAGTGTTGGAAGAAG-3′ and 5′-CTGCCCTCCAC GCAGAACCTC-3′ and sequenced.

Statistics. One-way analysis of variance (ANOVA) with the Bonferroni post hoc test was performed for the comparison of multiple groups using Prism software (GraphPad Software, Inc., San Diego, CA), and individual significance in the difference was calculated by two-tailed Student's or Welch's t test depending on whether variances of compared groups were regarded as equal or not. Correlation coefficients (R) were also calculated using the Prism software.

RESULTS

***APOBEC3* genotypes affect the kinetics of virus-neutralizing Ab production and early levels of plasma viremia.** To evaluate the possible effects of the *APOBEC3* polymorphisms on anti-FV B-cell responses, we first analyzed the kinetics of neutralizing Ab production and changes in plasma levels of viremia following FV inoculation in B6 mice possessing the disrupted *APOBEC3* gene ($mA3^{-/-}$) and their wild-type (WT) counterparts. FV-neutralizing Ab titers in the $mA3^{-/-}$ mice were significantly lower at 2 weeks postinfection than those in the WT mice, and this difference in Ab titers persisted throughout the 4 weeks of FV infection (Fig. 1A). However, Ab titers in the $mA3^{-/-}$ and WT mice became comparable at 5 weeks postinfection. Virus-neutralizing Abs detected in both groups of B6 mice were almost exclusively IgG. Thus, $mA3^{-/-}$ mice showed a significant delay in the initiation of virus-neutralizing Ab production. Plasma viral loads at PID 7 in the $mA3^{-/-}$ mice were on average 18-fold higher than those in the control WT mice; however, at PID 28 no viremia was detectable in both groups (Fig. 1B), in contrast to the previously observed persistence of viremia in $Rfv3^{s/s}$ mice at PIDs >30 (4, 5). These findings indicate that the B6-derived, resistance-associated $mA3^b$ allele not only restricts FV replication but also facilitates the production of FV-neutralizing Abs, which is consistent with previous findings (43, 49), except that FV-

neutralizing Abs can be produced, albeit more slowly, in the absence of $mA3^b$.

The *APOBEC3* transcripts are preferentially expressed in B cells, but Ab production in response to nonviral antigens is unaffected in APOBEC3-deficient mice. To address the mechanism by which the B6-derived APOBEC3 facilitates the production of virus-neutralizing Abs, we investigated the expression patterns of the *APOBEC3* gene in B6 mice. The *APOBEC3* transcripts were detected in abundance in the spleen and bone marrow (Fig. 2A). Further, we found that B cells more highly expressed the *APOBEC3* mRNA than T cells (Fig. 2B and C), possibly indicating a selective function of this enzyme in Ab formation.

The above finding led us to examine the possible effects of *APOBEC3* genotypes on the formation of B-cell repertoires, since the activation-induced cytidine deaminase (AID), one of the APOBEC family enzymes, is selectively expressed in B cells and functions as an essential initiator of both Ab class switching and somatic hypermutation (33). Thus, we first asked if a lack of the $mA3^b$ allele affects the production and class switching of Abs against nonviral antigens. The $mA3^{-/-}$ and WT B6 mice were immunized with DNP-OVA, a T-cell-dependent antigen, or DNP-Ficoll, a T-cell-independent antigen, and their anti-DNP Ab titers in sera were analyzed. As shown in Fig. 2D, $mA3^{-/-}$ mice responded to both antigens with specific IgM and IgG levels that were not different from those in the WT B6 mice. Thus, it is unlikely that APOBEC3 is directly required for the generation of antigen-specific B-cell repertoires and/or the differentiation of B cells into Ab-producing cells.

Efficient production of FV-neutralizing Abs from $mA3^b$-lacking B cells in the presence of viral-antigen-primed CD4$^+$ T cells. We next asked if the $mA3^b$-lacking B cells are selectively impaired in the recognition of FV antigens and/or differentiation into plasma cells capable of secreting virus-specific Abs. Our previous studies showed that a single immunization with an 18-mer peptide (peptide i) harboring a single CD4$^+$ T-cell epitope identified within the F-MuLV *env* gene product confers protective immunity to FV infection in susceptible $H2^{a/b}$ mice (17, 27). To examine if the presence of the resistance-associated $mA3^b$ allele is an absolute requirement for the production of FV-neutralizing Abs, F_1 hybrids between the $mA3^{-/-}$ or WT B6 and A/WySn mice that possessed the $mA3^{-/d}$ or $mA3^{b/d}$ genotype, respectively, were generated and immunized with peptide i, and the production of FV-neutralizing Abs and disease development following FV infection were analyzed. Consistent with our previous findings (49), nonimmunized $mA3^{-/d}$ mice exhibited higher hematocrit values, sustained after FV infection, and higher spleen weights at PID 77 than control $mA3^{b/d}$ mice (Fig. 3A), confirming that the B6-derived APOBEC3 can partially restrict FV-induced disease development. However, when the $mA3^{-/d}$ mice were immunized with peptide i prior to infection, FV-induced pathologies became barely detectable. Concomitantly, the levels of plasma viremia at PID 7 in the peptide-immunized $mA3^{-/d}$ mice were very low and were comparable to those observed in immunized $mA3^{b/d}$ mice, although the levels of viremia in nonimmunized $mA3^{-/d}$ mice were much higher than those in the nonimmunized WT mice (Fig. 3B). Of note, virus-neutralizing Ab titers at PID 14 in the immunized $mA3^{-/d}$ mice were as high as those in immunized $mA3^{b/d}$ mice (Fig. 3C). As the presence of virus-neutralizing Abs is a prerequisite for the prevention of FV-induced-disease development (4, 17), these results indicate that B cells lacking the resistance-associated

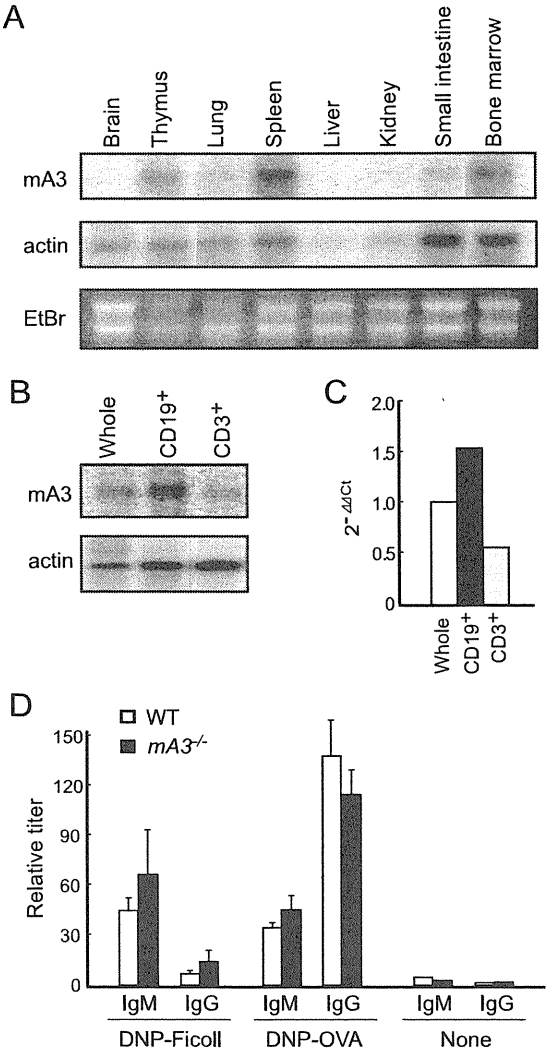

FIG. 2. Expression of *APOBEC3* mRNA in B cells and humoral immune responses against nonviral antigens in *APOBEC3*-deficient mice. (A and B) Expression levels of *APOBEC3* mRNA in the indicated tissues (A) or cells (B) prepared from B6 mice, as analyzed by Northern blotting. CD19$^+$ or CD3$^+$ cells were separated from the spleens of B6 mice by magnetic cell sorting. The RNA in agarose gels was visualized by ethidium bromide (EtBr) staining, and the β-actin gene was used as an internal control. (C) Expression levels of *APOBEC3* mRNA analyzed by quantitative real-time PCR assays. The relative expression levels of *APOBEC3* mRNA in each cell population were determined as $\Delta\Delta C_T$ relative to the values obtained with the whole spleen cells. Means for each cell type are shown. The experiments were performed twice with essentially identical results. (D) Antibody responses to nonviral antigens in *APOBEC3*-deficient B6 mice. $mA3^{-/-}$ and WT B6 mice were injected intraperitoneally (i.p.) with 100 μg of DNP-OVA in alum and boosted 10 days later with 50 μg of DNP-OVA without alum. T-cell-independent responses were elicited by i.p. injection of 100 μg DNP-Ficoll. Anti-DNP Ab titers of either IgM or IgG class in the sera before and at 7 days after the last immunization were measured by ELISA. The data shown here are the mean values of relative Ab titers determined with 4 to 6 separate serum samples and SEM.

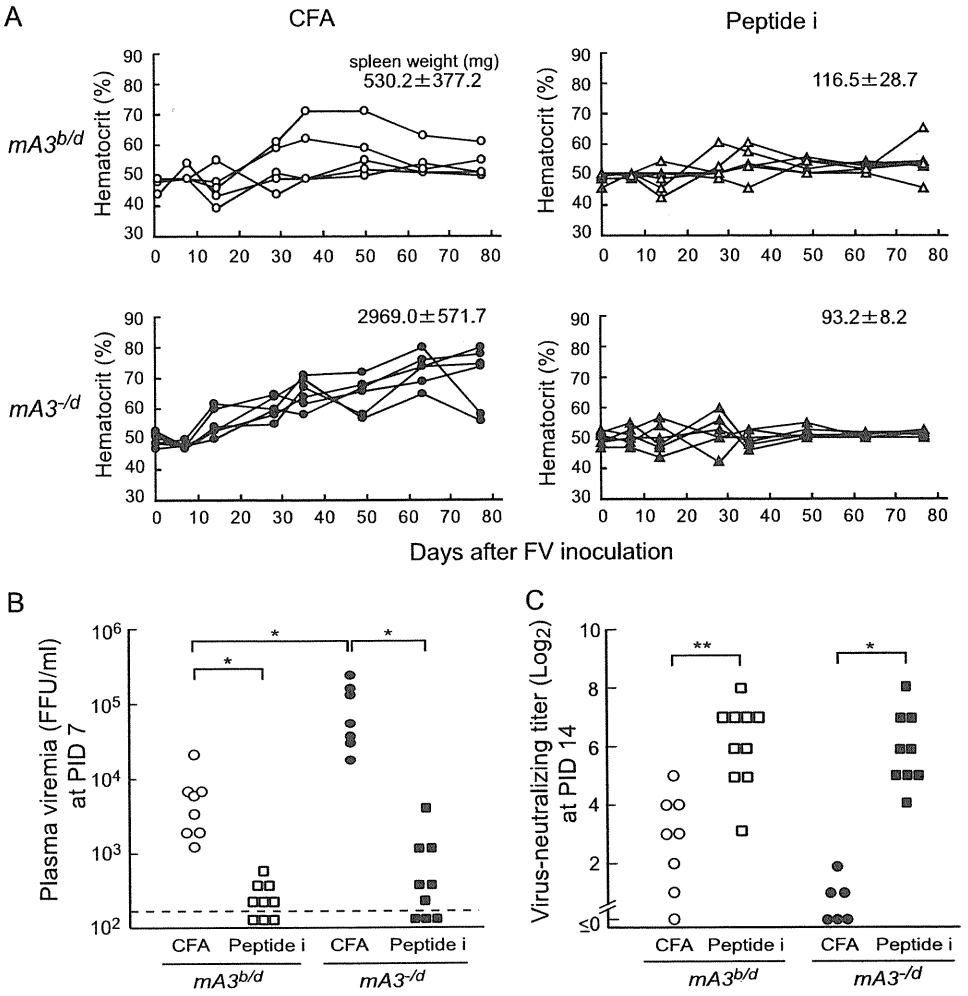

FIG. 3. Virus-neutralizing Ab responses in (B6 × A/WySn)F_1 mice possessing or lacking the *mA3*^{b} allele. (B6-*mA3*$^{b/b}$ × A/WySn)F_1 (*mA3*$^{b/d}$) and (B6-*mA3*$^{-/-}$ × A/WySn)F_1 (*mA3*$^{-/d}$) mice were immunized with 10 μg of peptide i emulsified with an equal volume of CFA or with CFA alone as a control, followed by infection with 1,500 SFFU FV. (A) Their hematocrit values were monitored following FV infection, and spleen weights (means ± SEM) were measured at PID 77. Each data point shows an actual hematocrit value detected from an individual mouse. (B and C) Plasma viral loads at PID 7 (B) and virus-neutralizing Ab titers of IgG plus IgM classes in the sera at PID 14 (C) were determined for each experimental group of mice. Each dot represents the actual value obtained from an individual mouse. The detection limit of plasma viremia was 200 FFU/ml. *, $P < 0.05$; **, $P < 0.005$ (by *t* test).

mA3^b allele are nevertheless able to produce levels of FV-neutralizing Abs that are sufficient to prevent the development of virus-induced pathologies in the presence of CD4$^+$ T cells primed with the viral antigen. Thus, mouse APOBEC3 does not appear to directly control the amounts and/or specificities of FV-neutralizing Abs, and the B-cell repertoire responsible for the recognition of FV-neutralizing epitopes develops in the absence of *mA3*^{b}.

Reduced production of neutralizing Abs in the *mA3*^{b}-deficient mice upon F-MuLV infection. Infection with the FV complex induces the growth and terminal differentiation of erythroid progenitor cells in mice possessing the *Fv2*^{s} allele. Therefore, it is possible that the skewed differentiation of myeloid cells into the erythroid compartment and/or physical derangements of cell-to-cell interactions in the spleen and bone marrow may impede the immune cell cooperation that is required for the production of virus-neutralizing Abs. In fact, due to the expression of SFFV gp55, the numbers of TER-119$^+$ erythroid cells in the spleen were massively increased in the *Fv2*$^{r/s}$ (B6 × A/WySn)F_1 mice (Fig. 3A and 4A). To eliminate the possible effect of erythroid cell proliferation on anti-FV immune responses, we utilized *Fv2*$^{r/r}$ B6 mice and infection with SFFV-free F-MuLV. Infection of B6 mice with FV complex induced a slight increase in the number of TER-119$^+$ erythroid cells, and this was significantly exacerbated in the absence of the *mA3*^{b} (Fig. 4A). Similar leakiness of the *Fv2*-associated resistance to FV-induced erythroid progenitor cell proliferation has been observed in B6 mice lacking T cells (11). On the other hand, infection with F-MuLV alone did not induce the growth of erythroid progenitor cells in either parental *Fv2*$^{r/r}$ or F_1 hybrid *Fv2*$^{r/s}$ mice regardless of the presence or absence of the *mA3*^{b} allele (Fig. 4A). Nevertheless, when infected with this nonpathogenic F-MuLV, the mice lacking the *mA3*^{b} allele exhibited significantly reduced production of neutralizing Abs compared with control mice harboring the *mA3*^{b} allele (Fig. 4B). Of note, the production of the IgG class

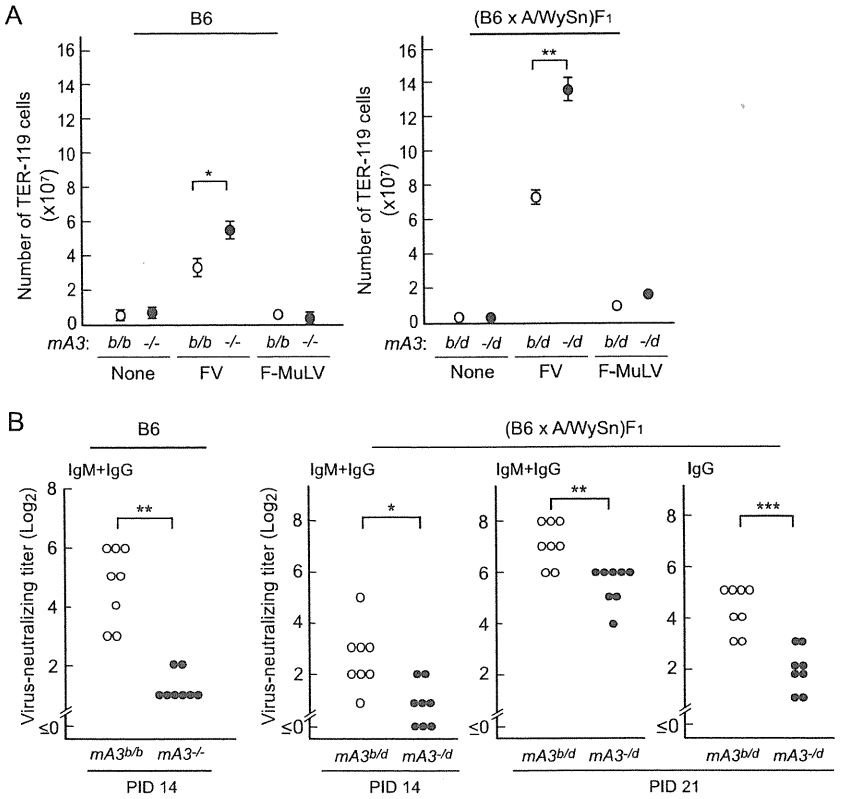

FIG. 4. Reduced levels of neutralizing Abs in mice lacking the $mA3^b$ allele following infection with nonpathogenic F-MuLV. (A) The $mA3^{-/-}$ and the WT $mA3^{b/b}$ B6 mice were infected with FV (10,000 SFFU) or F-MuLV (10,000 FFU), and (B6-$mA3^{-/-}$ × A/WySn)F_1 ($mA3^{-/d}$) and the control ($mA3^{b/d}$) mice were infected with 300 units of each virus. The numbers of TER-119$^+$ erythroid cells in the spleen at PID 10 were determined by fluorescence-activated cell sorter (FACS) analysis. Each dot represents the mean number of TER-119$^+$ cells calculated with 5 to 7 mice, and error bars indicate SEM. (B) Virus-neutralizing Ab titers following F-MuLV infection. Ab titers were analyzed at PID 14 in the B6 mice, while the neutralizing titers in the F_1 hybrid mice were compared at PIDs 14 and 21. Titers of IgG Abs at PID 21 were determined by treating each serum with 2-mercaptoethanol. Each dot represents the actual Ab titer obtained from an individual mouse. *, $P < 0.05$; **, $P < 0.005$; ***, $P < 0.0005$ (by t test).

of virus-neutralizing Abs was markedly delayed in the FV-susceptible (B6 × A/WySn)F_1 mice in the absence of the $mA3^b$ allele, suggesting that a lack of the $mA3^b$ allele influences not only the production but also the class switching of virus-neutralizing Abs in the absence of splenomegaly (Fig. 4B). These results indicate that the reduced production of virus-neutralizing Abs observed in the $mA3^b$-lacking mice is not due to the derangement of immune responses secondary to the exuberant growth of erythroid cells.

Inverse correlations between levels of viremia at PID 7 and virus-neutralizing Ab titers at PID 14. As infection with F-MuLV alone in the absence of splenomegaly caused delayed production of virus-neutralizing Abs in mice lacking the $mA3^b$ allele, we next explored if the replication of F-MuLV alone directly deranges the immune responses. Interestingly, when levels of viremia and titers of virus-neutralizing Abs were compared, we found a strong inverse correlation between viral loads at PID 7 and virus-neutralizing Ab titers at PID 14 in B6 mice possessing or lacking the $mA3^b$ allele, regardless of whether the virus inoculated was FV complex or F-MuLV alone (Fig. 5A). Similar results were also observed in (B6 × A/WySn)F_1 mice (Fig. 5B). These results suggest that effective early restriction of viral replication in the presence of B6-derived APOBEC3 might lead to a later improvement in virus-neutralizing Ab production. This notion is also consistent with the results shown in Fig. 3, where early control of viremia by peptide immunization resulted in higher titers of neutralizing Abs in the absence of the $mA3^b$. In other words, higher levels of neutralizing Abs might result from, rather than cause, the restriction of F-MuLV replication in the presence of the $mA3^b$ allele.

Higher viral loads in the absence of B6-derived APOBEC3 correlate with altered B-cell phenotypes. To evaluate the possible effects of F-MuLV infection on B-cell functions, we next analyzed possible alterations in the numbers and phenotypes of B cells in the spleens of $mA3^{-/-}$ B6 mice upon F-MuLV infection. The numbers of virus-infected cells expressing the F-MuLV gp70 were remarkably higher in the $mA3^{-/-}$ mice than in the WT counterparts at 10 days after F-MuLV infection (Fig. 6A), in agreement with previous data showing increased numbers of virus-producing cells in the $mA3^b$-lacking mice (49). Furthermore, we found significantly higher percentages of gp70$^+$ cells among splenic B cells in the $mA3^{-/-}$ mice than in the WT mice; around 10% of the splenic B cells from $mA3^{-/-}$ mice were gp70 positive, while very small fractions of B cells were gp70$^+$ in the WT mice (Fig. 6A). The total numbers of B cells detected as CD19$^+$ cells showed no significant differences between the $mA3^{-/-}$ and control B6 mice both

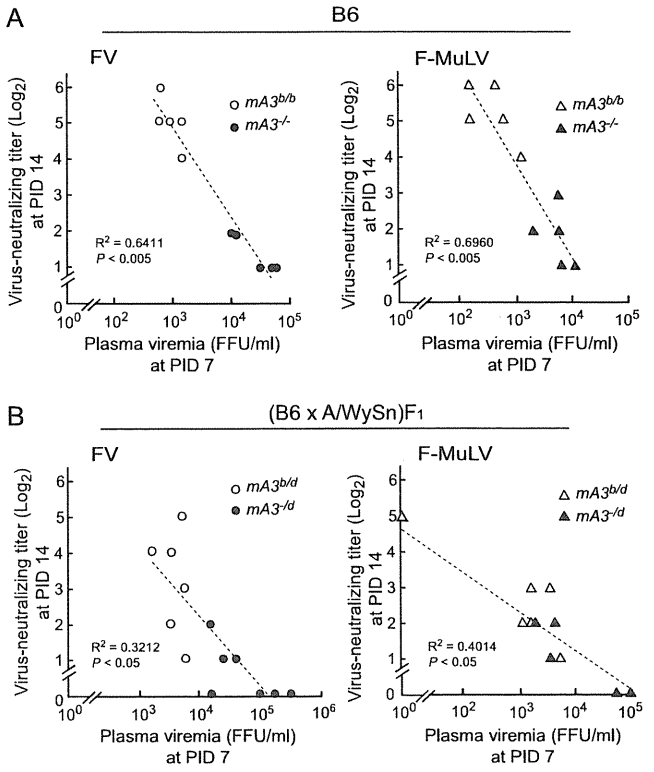

FIG. 5. Inverse correlations between plasma viral loads at PID 7 and neutralizing Ab titers at PID 14. (A) $mA3^{-/-}$ and WT $mA3^{b/b}$ B6 mice were infected with 10,000 units of either FV or F-MuLV. (B) $mA3^{-/d}$ and control $mA3^{b/d}$ F_1 hybrid mice were infected with 300 units of either virus. Each dot represents the actual level of plasma viremia and neutralizing Ab titer observed in an individual mouse.

before and at 10 days after F-MuLV infection (Fig. 6A). We next analyzed the expression of an activation marker on B cells and proportions of B-cell subpopulations in the spleen. Percentages of CD69-positive cells among splenic B cells were significantly higher in the $mA3^b$-deficient mice than in the WT mice after F-MuLV infection (Fig. 6B). Of note, the percentages of $CD69^+$ cells among splenic B cells directly correlated with the numbers of F-MuLV-infected splenic cells or of infected B cells, and the percentages of $CD69^+$ cells were higher among infected B cells than among gp70-negative B cells in $mA3^{-/-}$ mice (Fig. 6C and D), indicating that F-MuLV-infected B cells are preferentially activated. We further found that the absolute numbers of IgM^{high} IgD^{low} transitional B cells decreased, whereas the ratios of IgM^{low} IgD^{high} mature cells to IgM^{high} IgD^{low} transitional cells increased, in the $mA3^{-/-}$ mice following F-MuLV infection (Fig. 6E). Importantly, there were no significant changes in the numbers of B-cell populations in the WT mice upon F-MuLV infection (Fig. 6E). We also examined if F-MuLV infection influences B-lineage cell populations in the bone marrow, but there were no significant changes regardless of the *mA3* genotypes (data not shown). Taken together, the above data indicate that the rate of F-MuLV infection is directly associated with the levels of B-cell activation and proportions of B-cell subpopulations in the spleen, which may ultimately affect the production of virus-neutralizing Abs.

Polymorphism at the *BAFF-R* locus influences the persistence of viremia. Although the $mA3^{-/-}$ B6 mice showed higher levels of viremia than the WT mice at PID 7, they had cleared viremia by 4 weeks postinfection (Fig. 1B). This is apparently inconsistent with the previously observed phenotype of the $Rfv3^{s/s}$ mice, which continued to be viremic at >30 days following FV inoculation (5, 12). These observations led us to postulate that another locus within the mapped region on chromosome 15 might affect the persistence of viremia. In fact, the previous studies for the genetic mapping of the *Rfv3* locus were performed using A/WySn mice or their progeny obtained by crossing them with B10.A mice (5, 12, 16). Strain A/WySn is known to possess a natural mutation in the gene encoding BAFF-R, and it should be noted that the *BAFF-R* gene is located very close to the *APOBEC3* locus on chromosome 15 (16, 29). Therefore, we first reexamined our data on the genetic mapping of *Rfv3* performed using (B10.A × A/WySn)F_1 × A/WySn backcross mice (16). Among the mice that possessed a chromosomal recombination within or near the putative *Rfv3* locus, two mice (mice 1 and 2) in which both alleles of *BAFF-R* were derived from A/WySn mice ($BAFF\text{-}R^{mu}$) showed lower titers of virus-neutralizing Abs upon FV infection than those (mice 7 and 8) harboring a single allele of the B6-derived, wild-type *BAFF-R* ($BAFF\text{-}R^{wt/mu}$), even though all four mice were heterozygous for *APOBEC3* ($mA3^{b/d}$) (Fig. 7A). To evaluate the possible effect of *BAFF-R* genotypes on virus-neutralizing Ab production more decisively, we next used B6 mice harboring the disrupted *BAFF-R* gene and analyzed their virus-neutralizing Ab titers and plasma viral loads following FV infection. As expected, the $BAFF\text{-}R^{-/-}$ B6 mice showed lower titers of virus-neutralizing Abs at PID 14 and higher levels of plasma viremia at PID 7 than the WT counterparts (Fig. 7B and C) despite their $mA3^{b/b}$ genotype. More importantly, unlike the $mA3^{-/-}$, $BAFF\text{-}R^{wt/wt}$ mice, which had cleared viremia by PID 28 (Fig. 1B), 10 of the 13 FV-infected $BAFF\text{-}R^{-/-}$ mice were still viremic even at 28 days postinfection, while all 11 of the infected WT mice had cleared viremia ($P = 0.00015$, Fisher's exact test). Although $BAFF\text{-}R^{-/-}$ B6 mice possessed virus-neutralizing Abs at PID 28, their titers were significantly lower than those in the WT B6 mice and comparable to the levels of neutralizing titers in B6-$mA3^{-/-}$ mice at PID 21 (Fig. 1A and 7B). These results from the analysis using the gene-disrupted B6 mice indicate that the polymorphism at the *BAFF-R* locus, rather than that at *APOBEC3*, better explains the persistence of viremia at later stages of FV infection, the originally described *Rfv3* phenotype.

We also analyzed the levels of plasma viremia and neutralizing Ab titers in A/J mice possessing the wild-type *BAFF-R* gene and compared them with those in *BAFF-R*-mutated A/WySn mice. A/J mice showed significantly lower viral loads both at PID 7 and PID 28 and higher neutralizing Ab titers at PID 28 than A/WySn mice (Fig. 7D), although both A strains continued to be viremic at PID 28, probably due to their lack of the $mA3^b$ allele and resistant MHC haplotype, $H2^b$. In fact, it has been shown that the duration of viremia is prolonged (6) and Ab responses are delayed (28) in $H2^a$ mice in comparison with $H2^b$ mice even in the $Rfv3^{r/s}$ (B10 × A)F_1 background. These results, taken together, show that, regardless of *H2* haplotypes, a lack of the wild-type *BAFF-R* resulted in higher levels of viremia at PID 28.

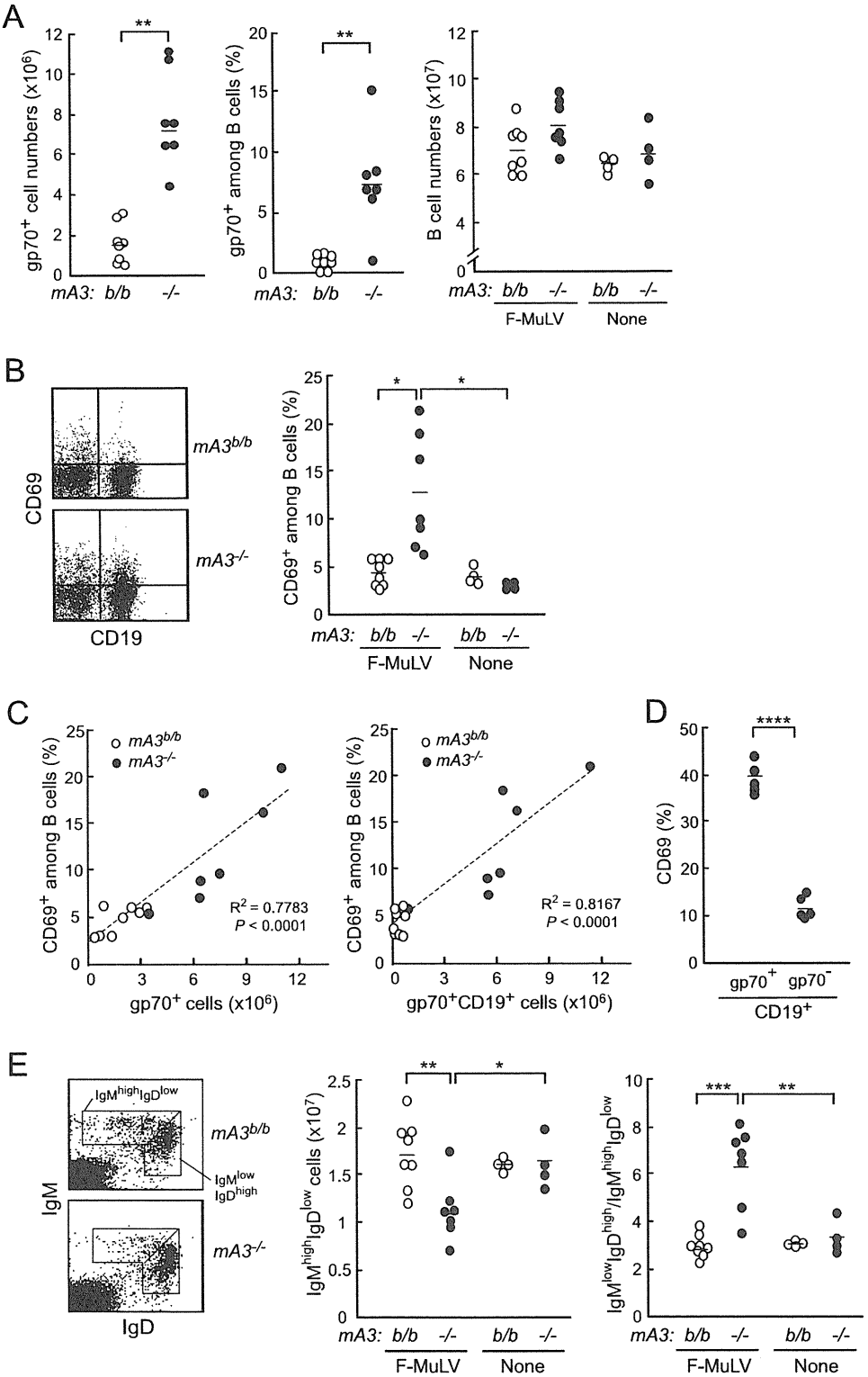

FIG. 6. Changes in phenotypes of peripheral B cells in the *mA3*$^{-/-}$ B6 mice following F-MuLV infection. Spleen cells were prepared from *mA3*$^{-/-}$ or WT B6 mice at 10 days after F-MuLV infection (10,000 SFFU). (A) Comparisons of the numbers of CD19$^+$ B cells and gp70$^+$ cells and the percentages of gp70$^+$ cells among B cells in the spleen between the *mA3*$^{-/-}$ and WT mice. (B) CD69 expression on the surfaces of splenic B cells. A representative pattern of CD69 expression on CD19$^+$ B cells in the spleen (left) and the percentages of CD69$^+$ cells among B cells before and 10 days after F-MuLV infection (right) are shown. (C) Correlations between the percentages of CD69$^+$ cells among B cells and the numbers of gp70$^+$ splenic cells or gp70$^+$ splenic B cells at PID 10. (D) Percentages of CD69$^+$ cells among gp70-positive or gp70-negative splenic B cells in the *mA3*$^{-/-}$ mice at PID 10. (E) Cell surface expression of IgM and IgD on splenocytes. Representative dot plots (left), the numbers of IgM^{high} IgD^{low} cells (middle), and the ratios of IgM^{low} IgD^{high} cells to IgM^{high} IgD^{low} cells (right) are shown. In the graphs in panels A, B, D, and E, each dot represents the actual value for the indicated cell population in a mouse, and horizontal bars represent the mean values for each group. *, $P < 0.05$; **, $P < 0.005$; ***, $P = 0.0001$; ****, $P < 0.00005$ (by *t* test).

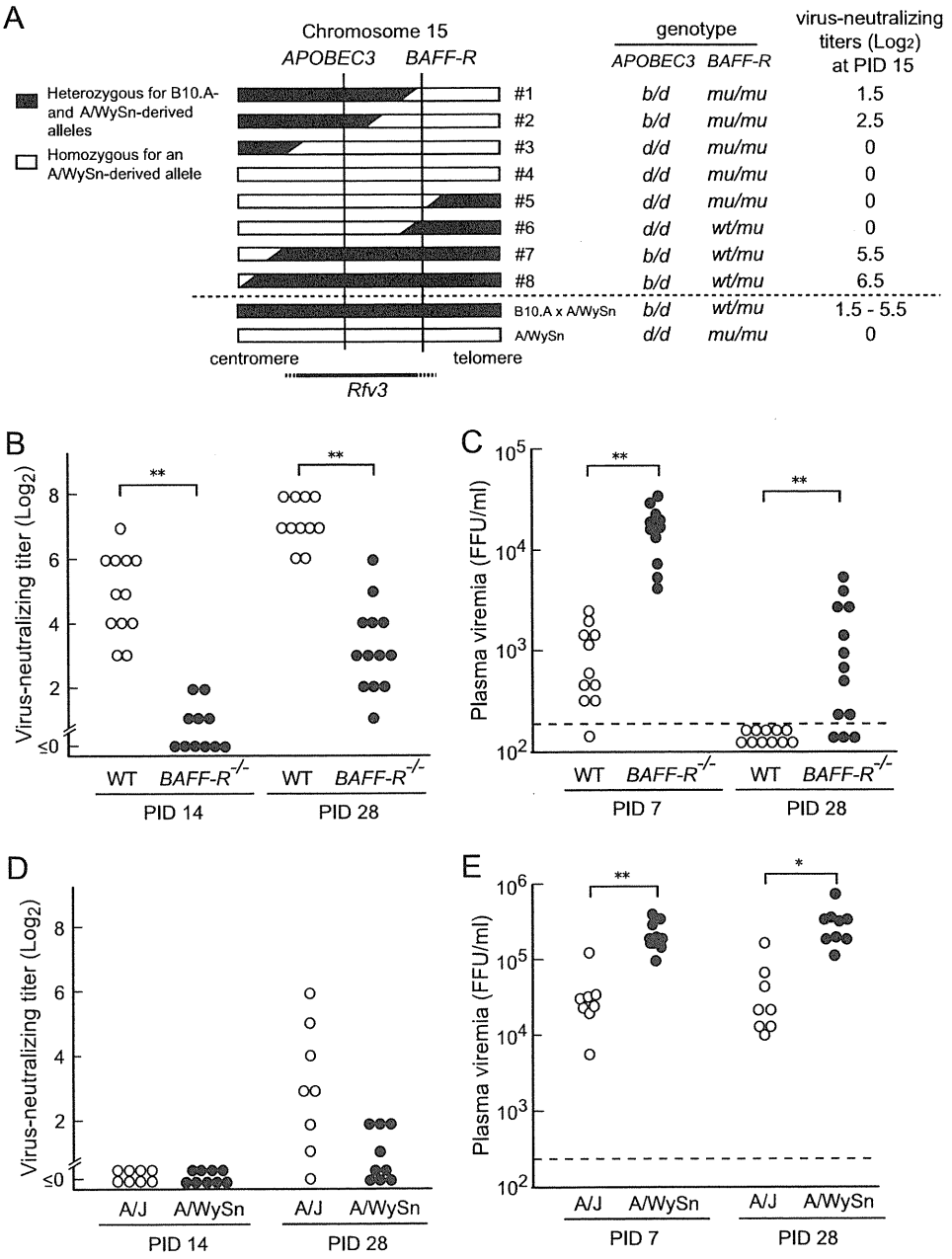

FIG. 7. Effects of polymorphisms at *BAFF-R* on FV-neutralizing Ab production and plasma viremia. (A) Linkage mapping of the *Rfv3* gene by using (B10.A × A/WySn) × A/WySn backcross mice (16). The genotypes of *APOBEC3* (*d*, A/WySn derived; *b*, B10.A derived) and *BAFF-R* (*mu*, A/WySn derived; *wt*, B10.A derived) for eight mice that possessed a recombination at the indicated region in chromosome 15 were determined by genome sequencing and PCR-based analyses, respectively,. The neutralizing Ab titers of these mice infected with 150 SFFU FV are shown at the right. (B and C) *BAFF-R*$^{-/-}$ and WT B6 mice were infected with 10,000 SFFU FV, and their plasma levels of viremia and virus-neutralizing Ab titers were analyzed by the same methods as described for Fig. 1. (D and E) A/WySn and A/J mice were infected with 1,500 SFFU FV, and the neutralizing Ab titers at PID 14 and PID 28 and plasma viral loads at PID 7 and PID 28 were analyzed. *, $P < 0.005$; **, $P < 0.0005$ (by *t* test).

Changes in B-cell phenotypes in *BAFF-R*$^{-/-}$ B6 mice upon F-MuLV infection. We next asked if the *BAFF-R*$^{-/-}$ B6 mice, like *mA3*$^{-/-}$ B6 mice, show alterations in activation and maturation phenotypes of B cells in the spleen after F-MuLV infection. As expected, both the numbers of gp70^{+} cells in the spleen and the percentages of gp70^{+} cells among splenic B cells were significantly higher in the *BAFF-R*$^{-/-}$ B6 mice at PID 10 than in the WT mice (Fig. 8A). Consistent with previous reports (1, 39, 51), both absolute numbers of mature B cells and ratios of IgM^{low} IgD^{high} mature cells to IgM^{high} IgD^{low} transitional cells were remarkably lower in the spleens of *BAFF-R*$^{-/-}$ B6 mice than in those of WT mice irrespective of F-MuLV infection (Fig. 8A and E). Following F-MuLV infection, the numbers of IgM^{high} IgD^{low} transitional B cells significantly decreased in comparison with those prior to infection in the *BAFF-R*$^{-/-}$ mice (Fig. 8E), as was observed in

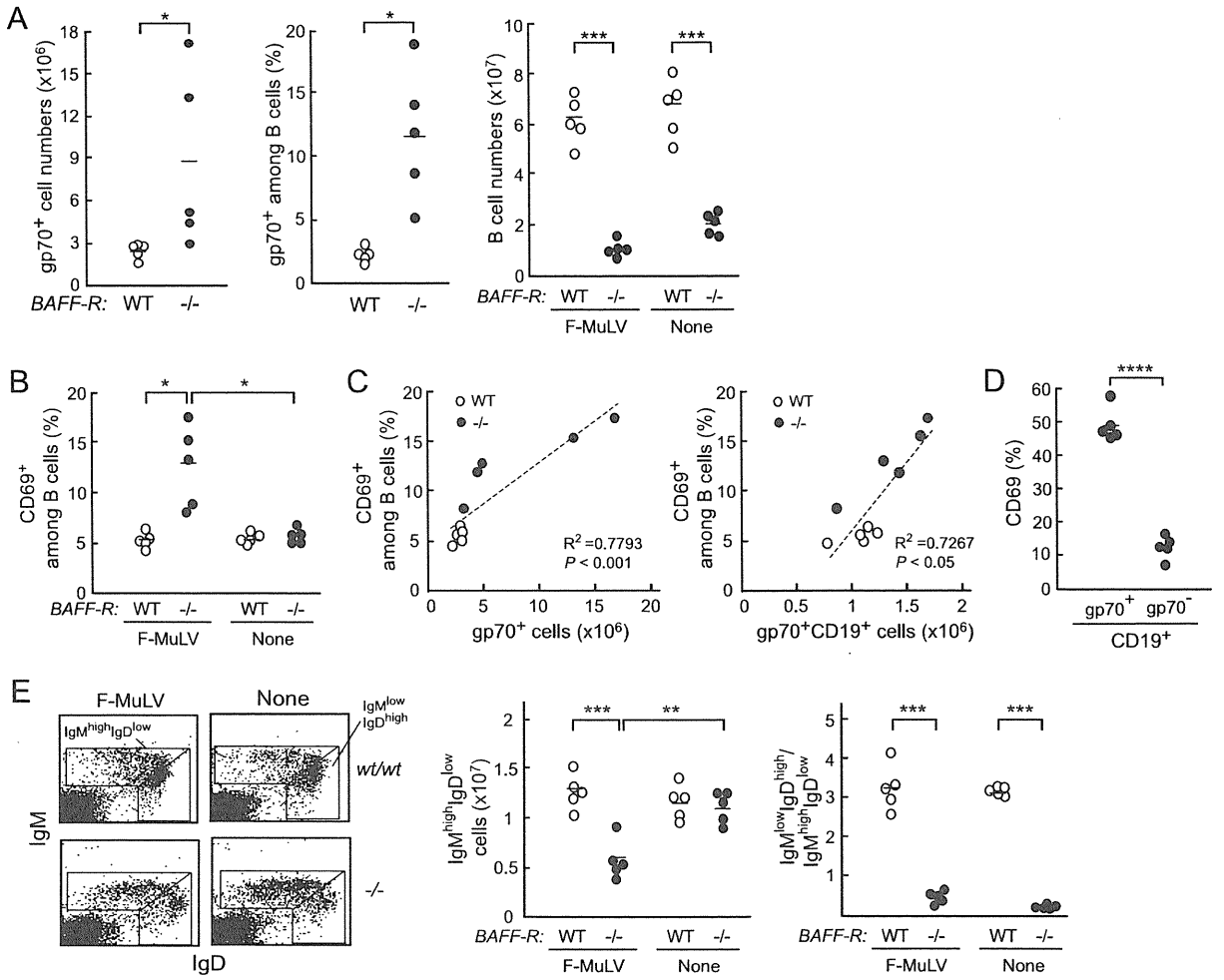

FIG. 8. Changes in phenotypes of peripheral B cells in the *BAFF-R*$^{-/-}$ B6 mice following F-MuLV infection. Spleen cells were prepared from *BAFF-R*$^{-/-}$ or WT B6 mice at 10 days after F-MuLV infection (10,000 SFFU). (A) Comparisons of the numbers of CD19$^+$ B cells and gp70$^+$ cells and percentages of gp70$^+$ cells among B cells in the spleen between the *BAFF-R*$^{-/-}$ and WT mice. (B) Percentages of CD69$^+$ cells among B cells before and 10 days after F-MuLV infection. (C) Correlations between the percentages of CD69$^+$ cells among splenic B cells and the numbers of gp70$^+$ splenic cells (left) or gp70$^+$ splenic B cells (right) at PID 10. (D) Percentages of CD69$^+$ cells among gp70-positive or gp70-negative splenic B cells at PID 10 in the *BAFF-R*$^{-/-}$ mice. (E) Cell surface expression of IgM and IgD on splenocytes. Representative dot plots (left), the numbers of IgM^{high} IgD^{low} cells (middle), and the ratios of IgM^{low} IgD^{high} cells to IgM^{high} IgD^{low} cells (right) are shown. In the graphs in panels A, B, D, and E, each dot represents the actual value for the indicated cell population in a mouse, and horizontal bars represent the mean values for each group. *, $P < 0.05$; **, $P < 0.005$; ***, $P < 0.0005$; ****, $P < 0.00005$ (by t test).

the *mA3*$^{-/-}$ mice (Fig. 6E). Furthermore, the percentages of CD69$^+$ cells among splenic B cells in the *BAFF-R*$^{-/-}$ mice were markedly higher at 10 days after F-MuLV infection than the percentages of those in the WT mice, and strong correlations between the percentages of CD69$^+$ cells among splenic B cells and the numbers of infected splenic cells or of infected splenic B cells were observed (Fig. 8B and C). In addition, higher percentages of gp70-positive B cells than of gp70-negative B cells were CD69 positive (Fig. 8D). These alterations in numbers and phenotypes of splenic B cells upon F-MuLV infection in the *BAFF-R*$^{-/-}$ mice were strikingly similar to those observed in the *mA3*$^{-/-}$ B6 mice (Fig. 6), indicating that higher viral loads developed either in the absence of *mA3*^{b} or in the absence of wild-type *BAFF-R* commonly result in the altered phenotypes of splenic B cells.

DISCUSSION

Infections with poorly cytopathic or noncytopathic viruses, including lymphocytic choriomeningitis virus (LCMV), hepatitis C virus, and human immunodeficiency virus (HIV), typically result in delayed formation of protective neutralizing Abs (3, 7, 42), while acutely cytopathic viruses are generally controlled by early production of virus-neutralizing Abs (52). Given that passive transfer of neutralizing Abs provides protection against chimeric simian-human immunodeficiency virus (SHIV) infection in macaque models (2, 13), understanding the mechanisms by which the production of neutralizing Abs is delayed in noncytopathic viral infections is important when considering successful vaccines to prevent and regulate persistent human viral infections, including that of HIV.

Friend virus provides a useful experimental model of per-

sistent infection with a noncytopathic virus. We and others have shown that the neutralizing Ab responses are important for both natural resistance to FV infection and effective vaccine-induced protection against FV (4, 8, 17, 24). The present study has demonstrated that the polymorphisms at the host loci *APOBEC3* and *BAFF-R*, each of which exhibits totally different physiological functions by encoding an intracellular cytidine deaminase or B-cell surface receptor for a survival factor, respectively, nevertheless affect the efficacies of virus-specific Ab responses against the retrovirus through strikingly similar mechanisms. We previously showed that polymorphisms at the *APOBEC3* locus directly influence both F-MuLV replication *in vitro* and the development of FV-induced pathogenesis *in vivo*; the APOBEC3 isoform highly expressed in the FV-resistant B6 strain of mice strongly inhibited virus replication and the development of FV-induced erythroid cell expansion (49). In the present study, we initially focused on the relationships between the *APOBEC3* genotypes and the kinetics of the production of virus-neutralizing Abs. Our findings indicated that the presence of the B6-derived $mA3^b$ allele is associated with rapid induction and class switching of F-MuLV-neutralizing Abs. As for the mechanisms by which the polymorphic APOBEC3 affects neutralizing Ab production, FV-induced growth of erythroid progenitor cells, which is more exuberant in the absence of the $mA3^b$ allele, is unrelated to reduced Ab production, since mice lacking the $mA3^b$ allele exhibited low neutralizing titers even upon infection with nonpathogenic F-MuLV (Fig. 4). Further, it is also unlikely that APOBEC3, as a DNA mutator, directly modifies B-cell repertoires, since we have found unaffected production and class switching of hapten-specific Abs following immunization with the T-independent and T-dependent forms of the antigen even in $mA3^b$-defficient B6 mice (Fig. 2). We also detected the early production of virus-neutralizing Abs from the $mA3^b$-lacking B cells upon priming of T helper cells (Fig. 3).

Intriguingly, we found a strong inverse correlation between the plasma viral loads at PID 7 and titers of neutralizing Abs at 2 weeks postinfection when both $mA3^b$-possessing and -lacking mice were analyzed as a group upon inoculation with either FV or F-MuLV (Fig. 5). The overall inverse correlation between the plasma levels of viremia at PID 7 and neutralizing Ab titers at PID 14 is not caused by the possible blockage of otherwise detectable neutralizing Abs by circulating viral particles, as serum samples were heat inactivated prior to the Ab assays to reduce the remaining infectivity due to viremia, if there was any, and neutralizing Abs were detectable even in the presence of high levels of viremia. In fact, in *BAFF-*$R^{-/-}$ B6 and A/J mice, significant titers of neutralizing Abs, comparable to the levels of those detected in WT B6 mice at PID 14, were detected in the presence of levels of viremia that were as high as or even higher than those in $mA3^{-/-}$ B6 mice at PID 7 (Fig. 7). Therefore, the possible presence of viremia does not explain the lack of detectable neutralizing titers at PID 14. Thus, these findings suggest that the levels of viral replication soon after FV infection affect the subsequent production of virus-specific Abs, rather than that virus-neutralizing Abs restrict the replication of the virus in the early phase. These notions are also consistent with the effect of T-helper-cell priming on the early production of virus-neutralizing Abs in the absence of $mA3^b$ (Fig. 3), as the numbers of virus-producing cells were drastically decreased 7 days after FV infection (27), even in the absence of B cells (17), in mice immunized with peptide i. Although further experiments are required, F-MuLV infection alone appears to impair virus-specific B-cell immune responses during the very early phase, which in turn results in the delayed and reduced production of virus-neutralizing Abs. In this context, in HIV-infected viremic individuals, both the cellular and humoral arms of the immune responses are unable to control the virus infection (10), and numerous studies have shown that B-cell dysfunction represents a central feature of HIV type 1 (HIV-1) infection (18, 30). The defective $CD4^+$ T-cell help may account for the observed B-cell abnormalities in HIV-1-infected individuals (54); however, since impaired B-cell functions have been observed early during HIV-1 infection, preceding the functional defects in $CD4^+$ T-cell activities (25, 50), the above HIV-induced B-cell dysfunction might be intrinsic. Infections with other viruses of a poorly cytopathic or noncytopathic nature, including hepatitis C virus and LCMV, also result in functional defects of B cells (3, 7, 14, 42).

As a possible link between early F-MuLV viremia and subsequent B-cell dysfunction, we found increased proportions of cells expressing the activation marker CD69 among splenic B cells in the $mA3^{-/-}$ mice compared to the WT mice after infection (Fig. 6). Further, the proportions of CD69-positive cells were in correlation with the numbers of virus-infected cells in the spleen. In HIV-infected individuals without long-term highly active antiretroviral therapy (HAART), a wide range of B-cell alterations, including increased polyclonal activation and enhanced expression of activation markers, have also been observed (7, 22, 23). Likewise, F-MuLV may directly induce hyperactivation and dysfunction of B cells. In addition, we also found increased ratios of mature to transitional B cells in the spleens of the APOBEC3-deficient B6 mice following F-MuLV infection. Transitional B cells, following F-MuLV infection, may rapidly differentiate into mature cells, undergo apoptosis, or change their location within the lymphoid organs. In this regard, a similar reduction in the number of transitional B cells was also observed upon F-MuLV infection in *BAFF-*$R^{-/-}$ mice (Fig. 8E), in which peripheral maturation of B cells is severely hampered (1, 20, 39, 51). Thus, it is more likely that transitional B cells are not differentiating into mature cells but are probably undergoing apoptosis in FV-infected mice. Indeed, HIV-infected individuals also exhibit abnormalities in B-cell subpopulations in their peripheral blood, including an increase in immature/transitional $CD10^+$ B cells and expansion by B cells with the CD27-negative exhausted phenotype (22, 31). Decreased survival of B cells has also been reported in both HIV-1 and simian immunodeficiency virus (SIV) infections (32, 38, 53). These abnormal phenotypes of B cells are likely to contribute to various facets of B-cell dysfunctions observed in several virus infections, including those currently demonstrated in F-MuLV infection. Consistent with this, earlier polyclonal hypergammaglobulinemia upon LCMV infection was correlated with delayed initiation of virus-neutralizing Ab responses (40). As B cells are definitively infected with F-MuLV in the absence of the $mA3^b$ allele (Fig. 6) and mouse APOBEC3 is expressed at higher levels in B cells than in T cells (Fig. 2), it is tempting to speculate that F-MuLV infection of B cells may directly impair their differentiation into Ab-secreting cells and/or the survival of antigen-stimulated pe-

TABLE 1. Genotypes of FV resistance loci and *Rfv3*-related phenotypes observed in the present study in different strains of mice

Mouse strain[a]	Genotype of:				Viremia[b] (FFU/ml) (SEM) at PID:		No of mice with virus-neutralizing Abs[c]/total no. tested at PID:	
	Fv2	*H2*	*APOBEC3*	*BAFF-R*	7	28	7	28
C57BL/6 (B6)	*r/r*	*b/b*	*b/b*	*wt/wt*	1,341 (319)	<133	21/22	17/17
B6-*mA3*$^{-/-}$	*r/r*	*b/b*	*−/−*	*wt/wt*	31,920 (7,200)	<133	0/9	10/10
B6-*BAFF-R*$^{-/-}$	*r/r*	*b/b*	*b/b*	*−/−*	16,309 (2,490)	2,458 (923)	0/11	9/13
A/WySn	*s/s*	*a/a*	*d/d*	*mu/mu*	239,978 (38,611)	353,544 (67,086)	0/9	0/9
A/J	*s/s*	*a/a*	*d/d*	*wt/wt*	36,438 (11,585)	42,000 (16,479)	0/8	5/8
(B6 × A/WySn)F_1	*r/s*	*b/a*	*b/d*	*wt/mu*	5,250 (1,729)	139 (6)	9/12	10/10
(B6-*mA3*$^{-/-}$ × A/WySn)F_1	*r/s*	*b/a*	*−/d*	*wt/mu*	79,157 (25,757)	7,328 (4,731)	0/10	12/12

[a] Homozygous $H2^b$ mice were infected with 10,000 SFFU of FV; $H2^{b/a}$ and $H2^{a/a}$ mice were infected with 1,500 SFFU of FV. All mice used are $Fv1^{b/b}$.
[b] Average levels of plasma viremia calculated with 8 to 22 mice.
[c] Numbers of mice with a neutralizing Ab titer of $\geq 2^3$.

ripheral B cells in the absence of the resistant *APOBEC3* genotype.

In addition to the effects of the APOBEC3 polymorphisms on Ab responses, we have also shown here that the polymorphisms at the *BAFF-R* gene located close to the *APOBEC3* locus on chromosome 15 influence the production of neutralizing Abs and the levels of plasma viremia in FV-infected mice. Among the progeny of (B10.A × A/WySn)F_1 mice backcrossed to A/WySn mice, the ones harboring only the A/WySn-derived *BAFF-R* mutant allele showed lower titers of virus-neutralizing Abs than those with a B10.A-derived allele. More importantly, most of the B6 mice lacking the functional *BAFF-R* allele possessed very low or undetectable levels of virus-neutralizing Abs at PID 14 and remained viremic at 28 days after infection with FV (Fig. 7); the latter phenotype differs from that of the *mA3*$^{-/-}$ mice and mimics the susceptible *Rfv3* phenotype originally observed in A/WySn mice and one-half of the (B10.A × A/WySn) × A/WySn backcross mice (5). In fact, in comparison with A/J mice that possess the wild-type *BAFF-R* gene, *BAFF-R*-mutant A/WySn mice showed extreme delays in neutralizing Ab production and much higher levels of viremia at PID 28 (Fig. 7). Thus, it appears that the *Rfv3* phenotypes defined by earlier neutralizing Ab production result from polymorphisms at both the *BAFF-R* and *APOBEC3* loci; on the other hand, the *Rfv3* phenotypes defined by persistent high-level viremia are predominantly influenced by the *BAFF-R* genotype (Table 1). It should be noted that the product of the mutant *BAFF-R* allele derived from A/WySn mice can interfere with the functions of the wild-type BAFF-R, and thus *BAFF-R*^{mu} and WT *BAFF-R* alleles are codominant (20, 39). Therefore, although (B6-*mA3*$^{-/-}$ × A/WySn)F_1 mice showed viremia in the absence of the *mA3*^{b} allele, this was observed in the condition of a reduced level of functional BAFF-R.

It is intriguing that the *mA3*^{b}-deficient mice and mice lacking the WT *BAFF-R* showed almost identical changes in B-cell subpopulations after F-MuLV infection (Fig. 6 and 8). In fact, IgM^{high} IgD^{low} transitional B cells decreased significantly at PID 10 in both *mA3*$^{-/-}$ and *BAFF-R*$^{-/-}$ B6 mice. As *APOBEC3* is preferentially expressed in B cells (Fig. 2) and a lack of *APOBEC3* resulted in significantly higher proportions of B cells that were infected and activated (Fig. 6), it is reasonable to postulate that in mice possessing the highly functional *mA3*^{b} allele APOBEC3 restricts F-MuLV replication in B cells and thereby preserves the functionality of B cells that produce virus-neutralizing Abs. However, in the case of BAFF-R, it is unlikely that this receptor is directly involved in the replication of F-MuLV in B cells. As BAFF-R-lacking B cells are short-lived (39, 45), the reduced survival of possibly F-MuLV-infected transitional B cells would result in reduced, rather than increased, levels of F-MuLV replication in *BAFF-R*$^{-/-}$ mice, even if transitional cells might be the preferential target of F-MuLV infection. Thus, the more likely explanation would be that some functions of mature B cells, most probably Ab production in response to F-MuLV antigens, are required for early containment of F-MuLV replication, and a lack of this early immune restriction in *BAFF-R*$^{-/-}$ mice results in more-rapid and extensive replication of F-MuLV in B cells, which in turn causes the excessive B-cell activation, disappearance of transitional B cells, and delayed production of neutralizing Abs. In this regard, it should be noted that the levels of plasma viremia were much lower in WT mice than in mice lacking functional BAFF-R even at 7 days after FV inoculation (Fig. 7), when virus-neutralizing Abs were not detectable in the serum (Fig. 1) (17, 27). Further, A/J mice possessed significantly lower levels of viremia than A/WySn mice at PID 7, even though virus-neutralizing Abs were still undetectable a week later, at PID 14 (Fig. 7D and E). These findings indicate that B-cell-associated immune responses may also function by 7 days postinfection in restricting FV replication. Since we have previously detected serum Abs capable of binding to the surfaces of FV-infected cells at PID 7 (17), the nonneutralizing anti-FV Abs may be involved in the restriction of FV replication observed at PID 7. Alternatively, neutralizing Abs locally active in the spleen and bone marrow, titers of which are below the level of detection in the sera, may restrict cell-to-cell FV propagation.

Finally, although levels of viremia were similarly high at PID 7 in the *mA3*^{b}- and *BAFF-R*-deficient mice, the titers of virus-neutralizing Abs gradually increased and viremia was cleared by PID 28 in *mA3*$^{-/-}$ mice in the presence of the wild-type *BAFF-R* (Fig. 1 and Table 1). Therefore, in addition to similar degrees of B-cell hyperactivation and presumable dysregulation of peripheral maturation of Ab-producing cells secondary to nonrestricted viral replication in the absence of the *mA3*^{b} or wild-type *BAFF-R* allele, the lack of functional BAFF-R itself

does contribute to the further delays in the control of viremia after PID 7. In fact, when *BAFF-R* is functional, virus-neutralizing Abs can be produced later even in the absence of $mA3^b$ and viremia can be reduced, as observed in A/J mice (Fig. 7). Although the presence or absence of viremia at PID 28 was also affected by genotypes at *mA3* and *H2*, as well as *BAFF-R*, loci in different strains of mice (Table 1), it is clear that genotypes at the *BAFF-R* locus alone produce an large difference in levels of viremia at PID 28, while the influence of the *mA3* genotypes on viremia at PID 28 can be observed only in the presence of the codominant $BAFF\text{-}R^{mu}$ allele. Thus, it is likely that the *Rfv3* phenotypes originally defined by persistence of viremia at PIDs >30 might be largely attributable to the effect of *BAFF-R* mutation in A/WySn mice.

ACKNOWLEDGMENTS

We thank M. Sakamoto for technical assistance and J. B. Dowell for critical reading and correction of the manuscript.

This work was supported in part by Grants-in-aid for Scientific Research from the Ministry of Education, Culture, Sports, Science and Technology of Japan, including the High-Tech Research Center project, and those from the Ministry of Health, Labor and Welfare of Japan for research on HIV/AIDS.

REFERENCES

1. **Amanna, I. J., J. P. Dingwall, and C. E. Hayes.** 2003. Enforced *bcl-xL* gene expression restored splenic B lymphocyte development in BAFF-R mutant mice. J. Immunol. **170**:4593–4600.
2. **Baba, T. W., V. Liska, R. Hofmann-Lehmann, J. Vlasak, W. Xu, S. Ayehunie, L. A. Cavacini, M. R. Posner, H. Katinger, G. Stiegler, B. J. Bernacky, T. A. Rizvi, R. Schmidt, L. R. Hill, M. E. Keeling, Y. Lu, J. E. Wright, T. C. Chou, and R. M. Ruprecht.** 2000. Human neutralizing monoclonal antibodies of the IgG1 subtype protect against mucosal simian-human immunodeficiency virus infection. Nat. Med. **6**:200–206.
3. **Battegay, M., D. Moskophidis, H. Waldner, M. A. Brundler, W. P. Fung-Leung, T. W. Mak, H. Hengartner, and R. M. Zinkernagel.** 1993. Impairment and delay of neutralizing antiviral antibody responses by virus-specific cytotoxic T cells. J. Immunol. **151**:5408–5415.
4. **Chesebro, B., M. Miyazawa, and W. J. Britt.** 1990. Host genetic control of spontaneous and induced immunity to Friend murine retrovirus infection. Annu. Rev. Immunol. **8**:477–499.
5. **Chesebro, B., and K. Wehrly.** 1979. Identification of a non-H-2 gene (*Rfv-3*) influencing recovery from viremia and leukemia induced by Friend virus complex. Proc. Natl. Acad. Sci. U. S. A. **76**:425–429.
6. **Chesebro, B., and K. Wehrly.** 1976. Studies on the role of the host immune response in recovery from Friend virus leukemia. I. Antiviral and antileukemia cell antibodies. J. Exp. Med. **143**:73–84.
7. **De Milito, A., A. Nilsson, K. Titanji, R. Thorstensson, E. Reizenstein, M. Narita, S. Grutzmeier, A. Sonnerborg, and F. Chiodi.** 2004. Mechanisms of hypergammaglobulinemia and impaired antigen-specific humoral immunity in HIV-1 infection. Blood **103**:2180–2186.
8. **Dittmer, U., D. M. Brooks, and K. J. Hasenkrug.** 1999. Requirement for multiple lymphocyte subsets in protection by a live attenuated vaccine against retroviral infection. Nat. Med. **5**:189–193.
9. **Doig, D., and B. Chesebro.** 1979. Anti-Friend virus antibody is associated with recovery from viremia and loss of viral leukemia cell-surface antigens in leukemic mice. Identification of Rfv-3 as a gene locus influencing antibody production. J. Exp. Med. **150**:10–19.
10. **Grossman, Z., M. Meier-Schellersheim, W. E. Paul, and L. J. Picker.** 2006. Pathogenesis of HIV infection: what the virus spares is as important as what it destroys. Nat. Med. **12**:289–295.
11. **Hasenkrug, K. J.** 1999. Lymphocyte deficiencies increase susceptibility to Friend virus-induced erythroleukemia in *Fv-2* genetically resistant mice. J. Virol. **73**:6468–6473.
12. **Hasenkrug, K. J., A. Valenzuela, V. A. Letts, J. Nishio, B. Chesebro, and W. N. Frankel.** 1995. Chromosome mapping of *Rfv3*, a host resistance gene to Friend murine retrovirus. J. Virol. **69**:2617–2620.
13. **Hessell, A. J., P. Poignard, M. Hunter, L. Hangartner, D. M. Tehrani, W. K. Bleeker, P. W. Parren, P. A. Marx, and D. R. Burton.** 2009. Effective, low-titer antibody protection against low-dose repeated mucosal SHIV challenge in macaques. Nat. Med. **15**:951–954.
14. **Hunziker, L., M. Recher, A. J. Macpherson, A. Ciurea, S. Freigang, H. Hengartner, and R. M. Zinkernagel.** 2003. Hypergammaglobulinemia and autoantibody induction mechanisms in viral infections. Nat. Immunol. **4**:343–349.
15. **Kabat, D.** 1989. Molecular biology of Friend viral erythroleukemia. Curr. Top. Microbiol. Immunol. **148**:1–42.
16. **Kanari, Y., M. Clerici, H. Abe, H. Kawabata, D. Trabattoni, S. L. Caputo, F. Mazzotta, H. Fujisawa, A. Niwa, C. Ishihara, Y. A. Takei, and M. Miyazawa.** 2005. Genotypes at chromosome 22q12-13 are associated with HIV-1-exposed but uninfected status in Italians. AIDS **19**:1015–1024.
17. **Kawabata, H., A. Niwa, S. Tsuji-Kawahara, H. Uenishi, N. Iwanami, H. Matsukuma, H. Abe, N. Tabata, H. Matsumura, and M. Miyazawa.** 2006. Peptide-induced immune protection of $CD8^+$ T cell-deficient mice against Friend retrovirus-induced disease. Int. Immunol. **18**:183–198.
18. **Lane, H. C., H. Masur, L. C. Edgar, G. Whalen, A. H. Rook, and A. S. Fauci.** 1983. Abnormalities of B-cell activation and immunoregulation in patients with the acquired immunodeficiency syndrome. N. Engl. J. Med. **309**:453–458.
19. **Lelie, P. N., H. W. Reesink, and C. J. Lucas.** 1987. Inactivation of 12 viruses by heating steps applied during manufacture of a hepatitis B vaccine. J. Med. Virol. **23**:297–301.
20. **Lentz, V. M., M. P. Cancro, F. E. Nashold, and C. E. Hayes.** 1996. *Bcmd* governs recruitment of new B cells into the stable peripheral B cell pool in the A/WySnJ mouse. J. Immunol. **157**:598–606.
21. **Lilly, F.** 1970. Fv-2: identification and location of a second gene governing the spleen focus response to Friend leukemia virus in mice. J. Natl. Cancer Inst. **45**:163–169.
22. **Malaspina, A., S. Moir, J. Ho, W. Wang, M. L. Howell, M. A. O'Shea, G. A. Roby, C. A. Rehm, J. M. Mican, T. W. Chun, and A. S. Fauci.** 2006. Appearance of immature/transitional B cells in HIV-infected individuals with advanced disease: correlation with increased IL-7. Proc. Natl. Acad. Sci. U. S. A. **103**:2262–2267.
23. **Martinez-Maza, O., E. Crabb, R. T. Mitsuyasu, J. L. Fahey, and J. V. Giorgi.** 1987. Infection with the human immunodeficiency virus (HIV) is associated with an in vivo increase in B lymphocyte activation and immaturity. J. Immunol. **138**:3720–3724.
24. **Messer, R. J., U. Dittmer, K. E. Peterson, and K. J. Hasenkrug.** 2004. Essential role for virus-neutralizing antibodies in sterilizing immunity against Friend retrovirus infection. Proc. Natl. Acad. Sci. U. S. A. **101**:12260–12265.
25. **Miedema, F., A. J. Petit, F. G. Terpstra, J. K. Schattenkerk, F. de Wolf, B. J. Al, M. Roos, J. M. Lange, S. A. Danner, J. Goudsmit, and P. T. A. Schellekens** 1988. Immunological abnormalities in human immunodeficiency virus (HIV)-infected asymptomatic homosexual men. HIV affects the immune system before $CD4^+$ T helper cell depletion occurs. J. Clin. Invest. **82**:1908–1914.
26. **Mikl, M. C., I. N. Watt, M. Lu, W. Reik, S. L. Davies, M. S. Neuberger, and C. Rada.** 2005. Mice deficient in APOBEC2 and APOBEC3. Mol. Cell. Biol. **25**:7270–7277.
27. **Miyazawa, M., R. Fujisawa, C. Ishihara, Y. A. Takei, T. Shimizu, H. Uenishi, H. Yamagishi, and K. Kuribayashi.** 1995. Immunization with a single T helper cell epitope abrogates Friend virus-induced early erythroid proliferation and prevents late leukemia development. J. Immunol. **155**:748–758.
28. **Miyazawa, M., J. Nishio, K. Wehrly, and B. Chesebro.** 1992. Influence of MHC genes on spontaneous recovery from Friend retrovirus-induced leukemia. J. Immunol. **148**:644–647.
29. **Miyazawa, M., S. Tsuji-Kawahara, and Y. Kanari.** 2008. Host genetic factors that control immune responses to retrovirus infections. Vaccine **26**:2981–2996.
30. **Moir, S., and A. S. Fauci.** 2009. B cells in HIV infection and disease. Nat. Rev. Immunol. **9**:235–245.
31. **Moir, S., J. Ho, A. Malaspina, W. Wang, A. C. DiPoto, M. A. O'Shea, G. Roby, S. Kottilil, J. Arthos, M. A. Proschan, T. W. Chun, and A. S. Fauci.** 2008. Evidence for HIV-associated B cell exhaustion in a dysfunctional memory B cell compartment in HIV-infected viremic individuals. J. Exp. Med. **205**:1797–1805.
32. **Moir, S., A. Malaspina, O. K. Pickeral, E. T. Donoghue, J. Vasquez, N. J. Miller, S. R. Krishnan, M. A. Planta, J. F. Turney, J. S. Justement, S. Kottilil, M. Dybul, J. M. Mican, C. Kovacs, T. W. Chun, C. E. Birse, and A. S. Fauci.** 2004. Decreased survival of B cells of HIV-viremic patients mediated by altered expression of receptors of the TNF superfamily. J. Exp. Med. **200**:587–599.
33. **Muramatsu, M., K. Kinoshita, S. Fagarasan, S. Yamada, Y. Shinkai, and T. Honjo.** 2000. Class switch recombination and hypermutation require activation-induced cytidine deaminase (AID), a potential RNA editing enzyme. Cell **102**:553–563.
34. **Ney, P. A., and A. D. D'Andrea.** 2000. Friend erythroleukemia revisited. Blood **96**:3675–3680.
35. **Ng, L. G., A. P. Sutherland, R. Newton, F. Qian, T. G. Cachero, M. L. Scott, J. S. Thompson, J. Wheway, T. Chtanova, J. Groom, I. J. Sutton, C. Xin, S. G. Tangye, S. L. Kalled, F. Mackay, and C. R. Mackay.** 2004. B cell-activating factor belonging to the TNF family (BAFF)-R is the principal BAFF receptor facilitating BAFF costimulation of circulating T and B cells. J. Immunol. **173**:807–817.
36. **Okeoma, C. M., J. Petersen, and S. R. Ross.** 2009. Expression of murine APOBEC3 alleles in different mouse strains and their effect on mouse mammary tumor virus infection. J. Virol. **83**:3029–3038.

37. **Persons, D. A., R. F. Paulson, M. R. Loyd, M. T. Herley, S. M. Bodner, A. Bernstein, P. H. Correll, and P. A. Ney.** 1999. *Fv2* encodes a truncated form of the Stk receptor tyrosine kinase. Nat. Genet. **23:**159–165.
38. **Peruchon, S., N. Chaoul, C. Burelout, B. Delache, P. Brochard, P. Laurent, F. Cognasse, S. Prevot, O. Garraud, R. Le Grand, and Y. Richard.** 2009. Tissue-specific B-cell dysfunction and generalized memory B-cell loss during acute SIV infection. PLoS One **4:**e5966.
39. **Rahman, Z. S., S. P. Rao, S. L. Kalled, and T. Manser.** 2003. Normal induction but attenuated progression of germinal center responses in BAFF and BAFF-R signaling-deficient mice. J. Exp. Med. **198:**1157–1169.
40. **Recher, M., K. S. Lang, A. Navarini, L. Hunziker, P. A. Lang, K. Fink, S. Freigang, P. Georgiev, L. Hangartner, R. Zellweger, A. Bergthaler, A. N. Hegazy, B. Eschli, A. Theocharides, L. T. Jeker, D. Merkler, B. Odermatt, M. Hersberger, H. Hengartner, and R. M. Zinkernagel.** 2007. Extralymphatic virus sanctuaries as a consequence of potent T-cell activation. Nat. Med. **13:**1316–1323.
41. **Robertson, M. N., M. Miyazawa, S. Mori, B. Caughey, L. H. Evans, S. F. Hayes, and B. Chesebro.** 1991. Production of monoclonal antibodies reactive with a denatured form of the Friend murine leukemia virus gp70 envelope protein: use in a focal infectivity assay, immunohistochemical studies, electron microscopy and western blotting. J. Virol. Methods **34:**255–271.
42. **Rosa, D., G. Saletti, E. De Gregorio, F. Zorat, C. Comar, U. D'Oro, S. Nuti, M. Houghton, V. Barnaba, G. Pozzato, and S. Abrignani.** 2005. Activation of naive B lymphocytes via CD81, a pathogenetic mechanism for hepatitis C virus-associated B lymphocyte disorders. Proc. Natl. Acad. Sci. U. S. A. **102:**18544–18549.
43. **Santiago, M. L., M. Montano, R. Benitez, R. J. Messer, W. Yonemoto, B. Chesebro, K. J. Hasenkrug, and W. C. Greene.** 2008. *Apobec3* encodes *Rfv3*, a gene influencing neutralizing antibody control of retrovirus infection. Science **321:**1343–1346.
44. **Sasaki, Y., S. Casola, J. L. Kutok, K. Rajewsky, and M. Schmidt-Supprian.** 2004. TNF family member B cell-activating factor (BAFF) receptor-dependent and -independent roles for BAFF in B cell physiology. J. Immunol. **173:**2245–2252.
45. **Shulga-Morskaya, S., M. Dobles, M. E. Walsh, L. G. Ng, F. MacKay, S. P. Rao, S. L. Kalled, and M. L. Scott.** 2004. B cell-activating factor belonging to the TNF family acts through separate receptors to support B cell survival and T cell-independent antibody formation. J. Immunol. **173:**2331–2341.
46. **Sitbon, M., B. Sola, L. Evans, J. Nishio, S. F. Hayes, K. Nathanson, C. F. Garon, and B. Chesebro.** 1986. Hemolytic anemia and erythroleukemia, two distinct pathogenic effects of Friend MuLV: mapping of the effects to different regions of the viral genome. Cell **47:**851–859.
47. **Sugahara, D., S. Tsuji-Kawahara, and M. Miyazawa.** 2004. Identification of a protective $CD4^+$ T-cell epitope in $p15^{gag}$ of Friend murine leukemia virus and role of the MA protein targeting the plasma membrane in immunogenicity. J. Virol. **78:**6322–6334.
48. **Super, H. J., K. J. Hasenkrug, S. Simmons, D. M. Brooks, R. Konzek, K. D. Sarge, R. I. Morimoto, N. A. Jenkins, D. J. Gilbert, N. G. Copeland, W. Frankel, and B. Chesebro.** 1999. Fine mapping of the Friend retrovirus resistance gene, *Rfv3*, on mouse chromosome 15. J. Virol. **73:**7848–7852.
49. **Takeda, E., S. Tsuji-Kawahara, M. Sakamoto, M. A. Langlois, M. S. Neuberger, C. Rada, and M. Miyazawa.** 2008. Mouse APOBEC3 restricts Friend leukemia virus infection and pathogenesis in vivo. J. Virol. **82:**10998–11008.
50. **Terpstra, F. G., B. J. Al, M. T. Roos, F. De Wolf, J. Goudsmit, P. T. Schellekens, and F. Miedema.** 1989. Longitudinal study of leukocyte functions in homosexual men seroconverted for HIV: rapid and persistent loss of B cell function after HIV infection. Eur. J. Immunol. **19:**667–673.
51. **Thompson, J. S., S. A. Bixler, F. Qian, K. Vora, M. L. Scott, T. G. Cachero, C. Hession, P. Schneider, I. D. Sizing, C. Mullen, K. Strauch, M. Zafari, C. D. Benjamin, J. Tschopp, J. L. Browning, and C. Ambrose.** 2001. BAFF-R, a newly identified TNF receptor that specifically interacts with BAFF. Science **293:**2108–2111.
52. **Thomsen, A. R., A. Nansen, C. Andersen, J. Johansen, O. Marker, and J. P. Christensen.** 1997. Cooperation of B cells and T cells is required for survival of mice infected with vesicular stomatitis virus. Int. Immunol. **9:**1757–1766.
53. **Titanji, K., F. Chiodi, R. Bellocco, D. Schepis, L. Osorio, C. Tassandin, G. Tambussi, S. Grutzmeier, L. Lopalco, and A. De Milito.** 2005. Primary HIV-1 infection sets the stage for important B lymphocyte dysfunctions. AIDS **19:**1947–1955.
54. **Wolthers, K. C., S. A. Otto, S. M. Lens, R. A. Van Lier, F. Miedema, and L. Meyaard.** 1997. Functional B cell abnormalities in HIV type 1 infection: role of CD40L and CD70. AIDS Res. Hum. Retroviruses **13:**1023–1029.

AIDS RESEARCH AND HUMAN RETROVIRUSES
Volume 26, Number 10, 2010

DOI: 10.1089/aid.2010.0043

Suppression of CCR5-Tropic HIV Type 1 Infection by OX40 Stimulation via Enhanced Production of β-Chemokines

Reiko Tanaka,[1] Yoshiaki Takahashi,[2] Akira Kodama,[1] Mineki Saito,[1] Aftab A. Ansari,[2] and Yuetsu Tanaka[1]

Abstract

To elucidate the immunological role for the costimulatory molecule OX40 against the early stage of HIV-1 infection, fresh peripheral blood mononuclear cells (PBMCs) from normal donors were stimulated with immobilized anti-CD3 monoclonal antibody (mAb) together with soluble anti-CD28 mAb for 24 h, infected with CCR5-tropic (R5) HIV-1, and then cocultured in the presence or absence of OX40 ligand (OX40L). Results of these studied showed that OX40 stimulation led to a marked reduction in levels of p24, the frequency of intracellular $p24^+$ cells, as well as HIV-1-mediated syncytium formation. The suppression was reversed by anti-OX40L mAb. The mechanism underlying the R5 HIV-1 suppression was shown to be mediated in part by the CCR5-binding β-chemokines RANTES, MIP-1α, and MIP-1β, since the effect of the OX40 stimulation was reversed by a neutralizing antibody mixture against these three β-chemokines. Thus, OX40 stimulation enhanced the production of these CCR5-binding β-chemokines by the activated PBMCs and subsequently down-modulated CCR5 expression on the activated $CD4^+$ T cells. Taken together, the present data revealed a new role for OX40 in HIV-1 infection and documents the fact that OX40 stimulation suppresses the infection of primary activated PBMCs with R5 HIV-1 via enhanced production of R5 HIV-1 suppressing β-chemokines.

Introduction

OX40 IS A MEMBER OF THE TUMOR NECROSIS FACTOR (TNF) receptor superfamily, which includes molecules such as Fas, CD27, CD30, CD40, 4-1BB, and others.[1,2] OX40 is transiently expressed on the cell surface of activated $CD4^+$ and $CD8^+$ T cells and select other lineages.[3–9] The ligand of OX40 (OX40L) was first described by our laboratory as gp34, which is preferentially expressed on the cell surface of human cell lines transformed by human T cell leukemia virus type I (HTLV-I).[10] Subsequently gp34 was cloned,[11] and finally identified as human OX40L that belongs to the TNF superfamily.[12] It is now clear that functional OX40L can be induced on a wide variety of cell lineages that include not only antigen presenting cells (APC) such as activated dendritic cells (DCs),[13] macrophages, and B cells,[14] but also select non-APC such as endothelial cells,[15] activated T cells,[16,17] NK cells,[18] and mast cells,[19] highlighting the multicell lineage expression of the OX40L molecule. Thus, it is reasoned that OX40-induced T cell costimulation in fact occurs quite frequently via OX40–OX40L interaction at sites of antigen stimulation and inflammation, resulting in modulation of immune responses. Such costimulation has been reported to result in the enhanced production of various cytokines such as interleukin (IL)-2, IL-4, IL-5, IL-6, IL-8, IL-13, and TNF-α,[20–23] and long-term survival of antigen-specific $CD4^+$ memory effector T cells.[9,24] Furthermore, the interaction between OX40 and OX40L promotes cell adhesion, which may facilitate T cell costimulation.[15] In contrast to these stimulatory profiles, it is of interest to note that high affinity interaction between OX40 and OX40L appears to result in apoptosis of OX40-expressing T cell lines and primary $CD4^+$ T cells under Th1 conditions.[25] These findings suggest that the interaction between OX40L and OX40 may control the fate of T cell responses with a double-edged effector mechanism.

It is not clear at present how OX40-mediated costimulation affects HIV-1 infection. Based on cell tropism, human immunodeficiency virus type 1 (HIV-1) isolates are classified into two main groups, CCR5-tropic (R5) and CXCR4-tropic (X4) strains.[26] The predominant HIV-1 strains isolated during acute infection are R5 tropic and often evolve to more pathogenic X4 strains as the disease progresses.[27] Despite these differences in tropism, both R5 and X4 HIV-1 strains are able to productively infect primary activated human $CD4^+$ T cells. We have previously shown that OX40 stimulation enhances X4 HIV-1 production in primary activated $CD4^+$ T cells and

[1]Department of Immunology, Graduate School of Medicine, University of the Ryukyus, Okinawa, Japan.
[2]Department of Pathology and Laboratory Medicine, Emory University School of Medicine, Atlanta, Georgia.

T cell lines via activation of the NF-κB pathway.[28] These observations prompted us to determine the role of OX40 costimulation on R5 HIV-1 infection. We report herein that in contrast to X4 HIV-1 infection, OX40 stimulation interferes with R5 HIV-1 infection by enhanced production of the R5 HIV-1-inhibiting β-chemokines.

Materials and Methods

Reagents

The medium used consisted of RPMI 1640 medium (Sigma-Aldrich. Inc., St. Louis, MO), supplemented with 10% fetal calf serum (FCS), 100 U/ml of penicillin, and 100 μg/ml of streptomycin (hereinafter called RPMI medium). Antihuman CD3 (clone OKT-3) and anti-CD28 monoclonal antibodies (mAbs) were purchased from the American Type Culture Collection (Rockville, MD) and Biolegend (San Diego, CA), respectively. Neutralizing mAbs against human RANTES, MIP-1α, and MIP-1β were purchased from R&D systems (Minneapolis, MN). The mAbs produced in our laboratory included mouse IgG1 mAbs anti-OX40L (clone 5A8),[29] antihuman OX40 (clone B-7B5),[28] anti-HIV-1 p24 (clones NP24 and 2C2) (Tanaka *et al.*, unpublished), anti-CD25 (clone H-8),[30] and anti-HTLV-I tax (clone TAXY-8)[31] as well as rat IgG2b mAbs anti-OX40 (clone W4-54)[32] and isotype control anti-HCV (clone Mo-8).[33] The in-house mAbs were purified from BALB/c or CB.17-SCID mouse ascites fluids by a gel filtration method. Some of them were labeled using FITC, Cy5, or HRP using commercial labeling kits (Dojin or Amersham, Japan) according to the manufacture's instructions. Biotinylated recombinant soluble human OX40 (sOX40 in a form of murine IgG2a-Fc fusion protein) and OX40L (sOX40L in a form of murine CD8-fusion protein) were purchased from Ancell (Bayport, MN) and used with FITC-streptavidin (Biolegend) for staining. Unlabeled glycosylated recombinant human OX40L, which consists of OX40L and human CD33 signal peptide produced in NS1 cells, was purchased from R&D systems. The mock-transfected CEM cell line (CEM/mock) and CEM cell line transfected with human OX40L (CEM/gp34) and shown to express OX40L[25] were used for some of the studies described below.

HIV-1 preparation

HIV-1_{JR-FL} and HIV-1_{NL4-3} viral stocks were produced by transfection of the 293T cells with the appropriate HIV-1 infectious plasmid DNAs utilizing the calcium phosphate method followed by *in vitro* culture of the transfected cells in RPMI medium for 2 and 3 days followed by collection of the supernatant fluid and virus isolation and purification as described previously.[34]

Quatitation of HIV-1 antigen and chemokines

Production of HIV-1 was determined by the measurement of HIV-1 core p24 levels produced in the culture supernatants using a commercial ELISA kit (Retrotec, Buffalo, NY) or our in-house formulated and standardized kits using a pair of anti-p24 mAbs of mouse origin with a detection limit of p24 of 2 pg/ml (Tanaka, unpublished). The levels of the human β-chemokines RANTES, MIP-1α, and MIP-1β in the culture supernatants were determined using ELISA kits purchased from Biosource (Camarillo, CA).

Stimulation of PBMCs in vitro and infection with HIV-1

PBMCs from healthy donors were stimulated as described previously.[17] Briefly, PBMCs obtained by density gradient centrifugation on HistoPAQUE-1077 (Sigma-Aldrich) were suspended at 2×10^6 cells/ml in RPMI medium, dispensed into individual wells of 24-well plates (BD) (1 ml/well) precoated with 5 μg/ml OKT3 for 1 h, and cultured in the presence of soluble 0.1 μg/ml anti-CD28 mAb. After cultivation at 37°C in a 5% CO_2 humidified atmosphere for 24 h, the activated PBMCs were washed once and infected with either R5 HIV-1_{JR-FL} or X4 HIV-1_{NL4-3} at a multiplicity of infection (moi) of 0.005 for 2 h as described previously.[34] After washing three times, PBMCs were resuspended at 1×10^6 cells/ml in RPMI medium, dispensed into individual wells of 48-well plates (BD) (0.5 ml/well), and cultured in the presence or absence of OX40L stimulation by either coculture with 2×10^5 cells/ml CEM/gp34 or by the addition of 1 μg/ml recombinant OX40L (rec.gp34). Syncytium formation was observed using an inverted microscope at a magnification of 200× as described previously.[35] In some experiments, 1-day-activated PBMCs were stimulated with 1 μg/ml recombinant OX40L for 24 h to examine the levels of chemokines in the culture supernatants.

Flow cytometry (FCM)

FCM analysis of live cells was carried out as described previously.[32] Briefly, cells to be analyzed were Fc-blocked with 2 mg/ml normal human pooled IgG on ice for 15 min. Aliquots of these cells were then subjected to staining using predetermined optimum concentrations of fluorescent dye-conjugated mAbs for 30 min on ice. The cells were then washed using FACS buffer (PBS containing 2% FCS and 0.1% sodium azide), fixed in 1% paraformaldehyde (PFA) containing FACS buffer, and analyzed using a FACS Calibur, and the data obtained were analyzed using the Cell Quest software (BD). To determine whether cell surface OX40 or OX40L is functional, aliquots of Fc-blocked cells were incubated with either biotinylated recombinant soluble OX40L or soluble OX40 at a concentration of 2.5 μg/ml for 30 min on ice, followed by staining with FITC-labeled streptavidin (Beckman Coulter) for 30 min on ice and then analyzed by FCM. For detection of HIV-1-infected cells, PBMCs were fixed with PBS containing 4% PFA followed by washing twice in FACS buffer containing 0.5% Triton X-100. These cells were Fc-blocked with 2 mg/ml normal human pooled IgG on ice for 15 min, and aliquots of these cells were stained with FITC- or Cy5-conjugated anti-HIV-1 p24 mAb (clone 2C2) for 30 min on ice. The cells were then washed using FACS buffer and absolute cell counts of $p24^+$ cells were performed by FCM using a cell counting kit (BD) according to the manufacturer's protocol.

Statistical analysis

Data were tested for significance using the Student's *t* test by using Prism software (GraphPad Software).

Results

Functional OX40 expression on $CD4^+$ T cells in primary activated PBMCs

To confirm that primary activated $CD4^+$ T cells express functional OX40 on their cell surface, fresh PBMCs from

healthy donors were stimulated *in vitro* with immobilized anti-CD3 mAb (OKT-3) along with soluble anti-CD28 mAb for 24 h and aliquots were stained with biotinylated recombinant OX40L (gp34) or OX40 followed by FITC-streptavidin or directly conjugated mAbs against OX40 and OX40L. As shown in Fig. 1A, two-thirds of $CD4^+$ T cells were positively stained with recombinant OX40L (gp34), indicating that these $CD4^+$ T cells expressed functional OX40. Similar percentages of $CD4^+$ T cells were also stained with anti-OX40 mAb. In the same culture, there were some $CD4^-$ cells that were stained with biotinylated OX40L (6.2% of total PBMCs) and anti-OX40 (9.7% of total PBMCs). These cells mainly consisted of $CD8^+$ T cells (data not shown). In the same activated PBMC culture, $OX40L^+$ cells as demonstrated by OX40 binding and anti-OX40L (gp34) staining were present at a low frequency, 1.1% and 0.6%, respectively. These $OX40L^+$ cells mainly consisted of activated $CD4^+$ and $CD8^+$ T cells, as reported previously,[32] suggesting that OX40-mediated costimulation of T cells may occur via T–T cell interaction initiated during an early period after PBMC activation.

A kinetic study of OX40 expression by primary activated PBMCs using anti-OX40 mAb (Fig. 1B) shows that the percent positive $OX40^+CD4^+$ T cells peaked on day 2, declined on day 3, and was reinduced by secondary stimulation and then gradually declined. After primary stimulation, the mean fluorescence intensity (MFI) of OX40 expression by $CD4^+$ T cells was highest on day 1 (MFI of 174) and declined on day 2 (MFI of 113) and day 3 (MFI of 64). The MFI following secondary stimulation peaked on day 1 and thereafter decreased to a stable level. The mean density of OX40 expression by $CD4^+$ T cells was two to three times higher than that of the non-$CD4^+$ (presumably $CD8^+$ T cells) at any stage of *in vitro* culture. In contrast, the expression level of CD25 (another activation marker) by the $CD4^+$ and the non-$CD4^+$ T cells was essentially similar throughout the culture period. These results showed that in the present experimental conditions, high levels of functional OX40 can be induced mainly on $CD4^+$ T cells in primary cultures of human PBMCs following activation, and its increased expression was transient as compared with CD25.

Effects of OX40 stimulation on R5 HIV-1 infection

To examine the effect of OX40 stimulation on infection of CCR5-tropic HIV-1, PBMCs activated for 24 h were infected with R5 HIV-$1_{JR\text{-}FL}$ at a low moi, and then were cocultured in the presence or absence of $OX40L^+$CEM cells (CEM/gp34) or recombinant soluble OX40L (rec.gp34). The reason for

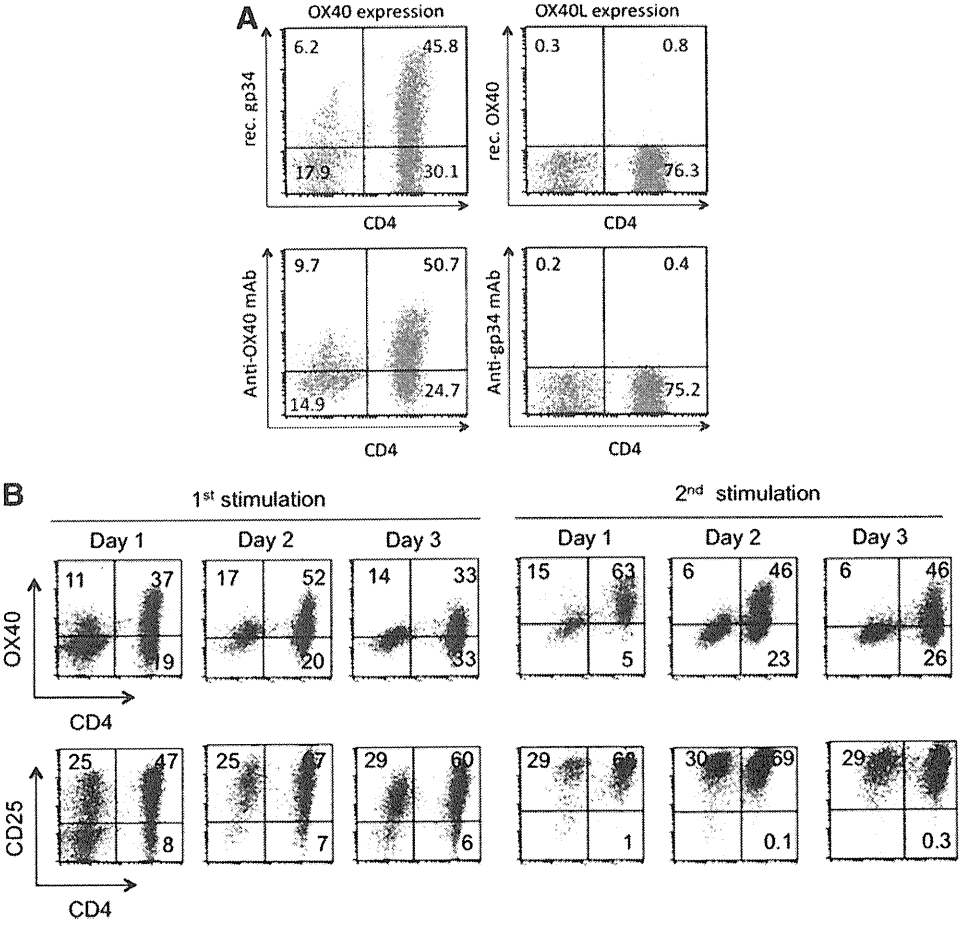

FIG. 1. Flow cytomeric analysis of OX40 and OX40L expression by anti-CD3/CD28-activated primary cultures of human PBMCs. (**A**) Fresh PBMCs were stimulated with immobilized OKT-3 in the presence of soluble anti-CD28 mAb for 24 h. Aliquots of these cells were examined for OX40 and OX40L expression by multicolor staining FCM using either (1) biotinylated recombinant OX40L (rec.gp34) followed by FITC-streptavidin and PE-anti-CD4 (top left), (2) Cy5-anti-OX40 and PE-anti-CD4 (bottom left), (3) biotinylated recombinant OX40 followed by FITC-streptavidin and PE-anti-CD4 (top right), or (4) Cy5-anti-OX40L (gp34) and PE-anti-CD4 (bottom right). (**B**) Kinetics of OX40 and CD25 expression by PBMCs following primary and secondary activation were examined by multicolor FCM using FITC-anti-OX40, PE-anti-CD4, and Cy5-anti-CD25. Secondary activation was performed on day 3 following primary stimulation. Data shown are representative of three independent experiments using three different donors.

choosing 1-day activated PBMCs as the target cells was because we wanted to study the response of $CD4^+$ T cells that were relatively naive to OX40L stimulation. In addition, we have previously shown that prolonged cultivation of activated PBMCs reduces the sensitivity of these cells to exogenous OX40L stimulation due to presensitization that may occur by endogenous OX40L expressed by T cells via T–T cell interactions.[32] As shown in Fig. 2A (top left), the production of HIV-1_{JR-FL} in the culture supernatants as shown by the levels of p24 was significantly reduced by coculture of activated PBMCs with CEM/gp34 ($p < 0.001$ on days 4 and 5) but not $OX40L^-$CEM (not shown). This inhibition was OX40 specific since the addition of the OX40L neutralizing mAb (clone 5A8) at coculture initiation reversed the inhibitory effect by OX40L stimulation ($p < 0.001$ on days 4 and 5). Furthermore, the addition of soluble recombinant OX40L at a concentration of 1 μg/ml also reduced the level of HIV-1 p24 production ($p < 0.01$ on days 4 and 5). The dose-response of the soluble OX40L is shown in Fig. 2A (top right), showing that the soluble OX40L at a concentration of more than 1 μg/ml suppressed R5 HIV-1 proliferation. It is worth noting that HIV-1_{JR-FL} often induces multinuclear giant cells (syncytia) in primary activated PBMCs, and that such syncytium formation was markedly inhibited by OX40 stimulation (Fig. 2B), suggesting that OX40 stimulation could interrupt the spread of R5 HIV-1 infection by inhibiting cell-to-cell interaction.

To determine whether the inhibition noted by OX40 stimulation was indeed due to blocking of the spread of HIV-1 to uninfected cells or secondary to inhibition of *de novo* production of HIV-1 from the infected cells, we examined the cell cultures for the frequency of intracellular HIV-1 core p24 antigen-positive cells in each culture. Figure 2C shows that the HIV-1 $p24Ag^+$ cell number per culture was significantly lower ($p < 0.001$) in the OX40-stimulated cultures than the control cultures. Again, the reduction was specifically reversed by the addition of anti-OX40L (gp34) mAb ($p < 0.001$). Together, these results clearly indicate that OX40 stimulation suppresses R5 HIV-1 infection in primary activated PBMCs

OX40 stimulation does not inhibit infection of X4 tropic HIV-1 in activated PBMCs

Our laboratory previously reported that X4 HIV-1 infection of primary $CD4^+$ T cells activated twice (day 0 and 3) was markedly enhanced by OX40 stimulation.[28] We therefore tested whether OX40 stimulation in the present culture conditions could modify infection of the day-1-activated PBMCs with X4 HIV-1. Thus, 1-day activated PBMCs were infected with X4 HIV-1_{NL4-3} and then cultured in the presence or absence of OX40 costimulation. As shown in Fig. 3, X4 HIV-1 infection was not blocked ($p < 0.001$ on days 3–5) or slightly enhanced by stimulation by coculture with OX40L-expressing $CD4^+$ T cells. These data suggest that the effect of OX40 stimulation on HIV-1 infection is distinct depending on the coreceptor tropism of HIV-1 strains.

CCR5-binding β-chemokines are involved in the R5 HIV-1 interference by OX40 stimulation

The present observations that OX40 stimulation interfered with R5 but not X4 HIV-1 infection of activated PBMCs

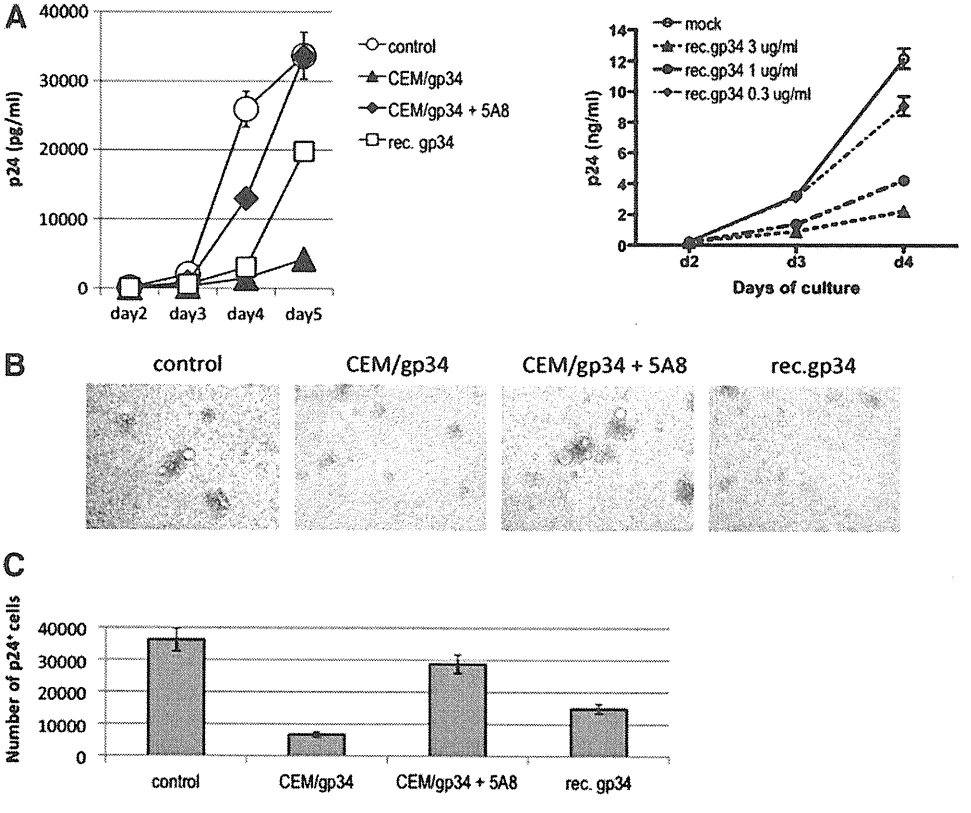

FIG. 2. Inhibition of R5 HIV-1 replication by OX40 stimulation *in vitro*. (**A**) Fresh PBMCs stimulated as in Fig. 1 for 24 h were infected with HIV-1_{JR-FL}, washed, and then cocultured in the presence or absence of OX40L-expressing cells (CEM/gp34) or 1 μg/ml recombinant soluble OX40L (rec.gp34) (left panel), or at different doses (right panel). HIV-1 production in the culture supernatants was monitored daily by p24 ELISA. (**B**) HIV-1-induced syncytium formation in aliquots of the same infected PBMCs as in (**A**) was observed on day 4 after infection under an inverted microscope at a magnification of 200×. (**C**) Aliquots of the same infected PBMCs on day 5 postinfection were analyzed for frequencies of intracellular $p24^+$ cells using flow cytometry. Data shown are the absolute number of $p24^+$ cells in each culture condition and are representative data of five independent experiments using three different donors.

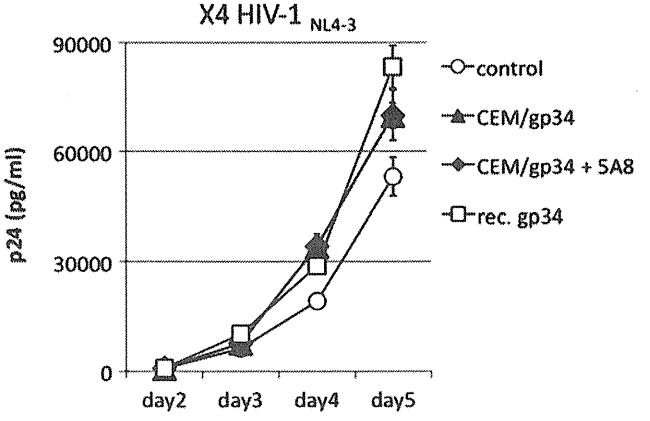

FIG. 3. OX40 stimulation does not inhibit X4 HIV-1 infection of activated PBMCs. Fresh primary anti-CD3/CD28-activated PBMCs were infected with X4 HIV-1_{NL4-3}, as described in Fig. 2, and production of HIV-1 was monitored by p24 ELISA. Data shown are representative of five independent experiments using three different donors.

prompted us to examine the factors that could potentially be involved and reasoned that the CCR5 binding β-chemokines were likely candidates. Therefore, studies were carried out using a mixture of neutralizing mAbs against RANTES, MIP-1α, and MIP-1β in efforts to determine if their addition could reverse the R5 HIV-1 inhibiting effect by OX40 stimulation. As shown in Fig. 4A, the OX40-mediated R5 HIV-1 suppression was significantly reversed by the addition of the mixture of antibodies ($p < 0.001$ on days 4 and 5). Interestingly, use of mAbs against the three individual β-chemokines in similar cultures performed in parallel did not show any detectable reversal of the effect of OX40 stimulation (data not shown), suggesting that all the three chemokines contributed in the suppression of R5 HIV-1 infection. To confirm that these β-chemokines were actually produced in the OX40-stimulated PBMCs, we quantitated the concentrations of the chemokines in the culture supernatants. Figure 4B shows that OX40 stimulation enhanced the production of these β-chemokines in the activated PBMCs ($p < 0.001$). Furthermore, after OX40 stimulation, the level of CCR5 expression on the cell surface of $CD4^+$ T cells in the activated PBMCs was significantly reduced (Fig. 4C). In contrast, CXCR4 expression by $CD4^+$ T cells was slightly up-regulated in the same OX40-stimulated PBMC culture. Therefore, these results indicate that OX40 stimulation can suppress R5 HIV-1 infection via enhanced production of CCR5-binding β-chemokines. The fact that the inhibition of R5 HIV-1 infection was reversed by the addition of antibodies against the β-chemokines suggests that the inhibition is not secondary to down-regulation of CCR5 but likely was due to the blocking of the CCR5 by the β-chemokines.

Discussion

In the present study, we showed for the first time that costimulation of primary activated PBMCs by OX40L reduced the productive infection with R5 HIV-1. This effect is distinct from the effect of OX40L-induced OX40 stimulation on infection by X4 HIV-1 in which OX40 enhances the infection.[28] The underlying mechanism for R5 HIV-1-restiriced suppression was shown to be enhanced production of the CCR5-binding β-chemokines that led to either blocking and/or down-modulation of CCR5 expression on activated $CD4^+$ T cells.

It has been reported that OX40 stimulation of activated T cells induces enhanced production of a variety of cytokines such as IL-2, IL-4, IL-5, IL-6, IL-8, IL-13, and TNF-α.[20–23] As far as we know there have been no reports on enhanced CCR5-binding β-chemokine production by activated PBMCs and CCR5 down-modulation in activated $CD4^+$ T cells by OX40 stimulation. The enhancement of each chemokine production increased in the order RANTES (sixfold), MIP-1β (~15-fold), and MIP-1α (~50-fold) (Fig. 4B). It is possible that the levels of chemokines quantitated in the culture supernatants were even higher since some of them might have been absorbed by CCR5-expressing cells. All three β-chemokines might be involved in R5 HIV-1 suppression since our preliminary data show that the mixture of all the three mAbs against the β-chemokines, but not single mAb against each chemokine, was required for complete reversal of the OX40-mediated R5 HIV-1 suppression in the present culture conditions (data not shown). Further studies need to be performed to determine whether it is indeed the direct result of $CD4^+$ T cell activation or due to synthesis by the other cell lineages present in the culture conditions employed. Data from our preliminary experiments show that the enhanced production of the three β-chemokines by OX40 stimulation was significantly reduced (>80%) after removal of both $CD4^+$ and $CD8^+$ T cells, and only partially after removal of $CD14^+$ monocytes, but not after removal of $CD19^+$ B cells (data not shown). Thus, it is possible that both $CD4^+$ and $CD8^+$ T cells and to a lesser extent monocytes are the major producers of these β-chemokines. Further studies including analysis of cells stained for cell surface markers coupled with intracellular staining for the chemokines in question are currently in progress.

Several lines of evidence suggest that targeting CCR5 by small chemical compounds, modified RANTES, or MIP-β is a promising therapy for HIV-1 infection not only for HARRT-naive patients but also for treatment-experienced patients infected with multidrug-resistant, CCR5-tropic HIV-1.[36–39] In addition, since R5 but not X4 HIV-1 strains are the major transmitters of primary HIV-1 infection,[26,27] the therapeutic targeting of CCR5 as a prophylaxis for HIV-1 prevention appears reasonable and appropriate. Thus, on the basis of the results of the present study it can be hypothesized that OX40 stimulation may have a therapeutic potential for the prevention of R5 HIV-1 infection. The choice of methods to activate $CD4^+$ T cells via the OX40 pathway will obviously be critical for optimal therapeutic benefit with the knowledge that such activation is a two-edged sword and thus strategies that include methods to finely regulate the extent and duration of OX40-mediated activation need to be identified. In this regard, the use of soluble recombinant human OX40L may be one approach since the concentration of the recombinant OX40L required for HIV-1 suppression was around 1 μg/ml (Fig. 2). Another strategy that has been utilized to increase the efficiency and bioactivity of OX40L involves the generation of multimeric forms of OX40L trimer molecules, which have been shown to be markedly more potent in IL-8 production using an OX40-exressing cell line.[23] Other strategies that may be worthwhile to investigate include the generation of viral